ICSNC 2021

The Sixteenth International Conference on Systems and Networks Communications

ISBN: 978-1-61208-895-2

October 3 -7, 2021

Barcelona, Spain

ICSNC 2021 Editors

Jorge Cobb, The University of Texas at Dallas, USA

Cosmin Dini, IARIA, USA/EU

ICSNC 2021

Forward

The Sixteenth International Conference on Systems and Networks Communications (ICSNC 2021), held October 3 - 7, 2021 in Barcelona, Spain, continued a series of events covering a broad spectrum of systems and networks related topics.

As a multi-track event, ICSNC 2021 served as a forum for researchers from the academia and the industry, professionals, standard developers, policy makers and practitioners to exchange ideas. The conference covered fundamentals on wireless, high-speed, mobile and Ad hoc networks, security, policy based systems and education systems. Topics targeted design, implementation, testing, use cases, tools, and lessons learnt for such networks and systems

The conference had the following tracks:

- TRENDS: Advanced features
- WINET: Wireless networks
- HSNET: High speed networks
- SENET: Sensor networks
- MHNET: Mobile and Ad hoc networks
- AP2PS: Advances in P2P Systems
- MESH: Advances in Mesh Networks
- VENET: Vehicular networks
- RFID: Radio-frequency identification systems
- SESYS: Security systems
- MCSYS: Multimedia communications systems
- POSYS: Policy-based systems
- PESYS: Pervasive education system

We welcomed technical papers presenting research and practical results, position papers addressing the pros and cons of specific proposals, such as those being discussed in the standard forums or in industry consortiums, survey papers addressing the key problems and solutions on any of the above topics, short papers on work in progress, and panel proposals.

We take here the opportunity to warmly thank all the members of the ICSNC 2021 technical program committee as well as the numerous reviewers. The creation of such a broad and high quality conference program would not have been possible without their involvement. We also kindly thank all the authors that dedicated much of their time and efforts to contribute to the ICSNC 2021. We truly believe that thanks to all these efforts, the final conference program consists of top quality contributions.

This event could also not have been a reality without the support of many individuals, organizations and sponsors. We also gratefully thank the members of the ICSNC 2021 organizing committee for their help in handling the logistics and for their work that is making this professional meeting a success. We gratefully appreciate to the technical program committee co-chairs that contributed to identify the appropriate groups to submit contributions.

We hope the ICSNC 2021 was a successful international forum for the exchange of ideas and results between academia and industry and to promote further progress in networking and systems communications research.

ICSNC 2021 Steering Committee

Marc Kurz, University of Applied Sciences Upper Austria, Faculty for Informatics, Communications and Media, Austria
Jin-Shyan Lee, National Taipei University of Technology (Taipei Tech.), Taiwan
Rony Kumer Saha, KDDI Research Inc., Japan
Eugen Borcoci, University Politehnica of Bucharest, Romania

ICSNC 2021 Publicity Chair

José Miguel Jiménez, Universitat Politecnica de Valencia, Spain
Lorena Parra, Universitat Politecnica de Valencia, Spain

ICSNC 2021

Committee

ICSNC 2021 Steering Committee

Marc Kurz, University of Applied Sciences Upper Austria, Faculty for Informatics, Communications and Media, Austria
Jin-Shyan Lee, National Taipei University of Technology (Taipei Tech.), Taiwan
Rony Kumer Saha, KDDI Research Inc., Japan
Eugen Borcoci, University Politehnica of Bucharest, Romania

ICSNC 2021 Publicity Chair

José Miguel Jiménez, Universitat Politecnica de Valencia, Spain
Lorena Parra, Universitat Politecnica de Valencia, Spain

ICSNC 2021 Technical Program Committee

Ahmed M. Abdelmoniem, KAUST, Saudi Arabia
Abdelkaher Ait Abdelouahad, Chouaib Doukkali University, Morocco
Baadache Abderrahmane, University of Benyoucef Benkhadda, Algeria
Ishtiaq Ahmad, University of South Australia, Australia
S. Arnaud R. M. Ahouandjinou, University of Abomey-Calavi (UAC) / Coastal Opal University (ULCO), France
Francisco Airton Silva, Universidade Federal do Piauí, Brazil
Alper Akarsu, HAVELSAN, Turkey
Pedro Ákos Costa, NOVA University of Lisbon & NOVALINCS, Portugal
Adel Aldalbahi, KFU College of Engineering, Saudi Arabia
Lina Alfantoukh, King Faisal Specialist Hospital & Research Centre, Riyadh, Saudi Arabia
Osama Aloqaily, University of Ottawa, Canada
Abdallah A. Alshehri, Saudi Aramco, Dhahran, Saudi Arabia
Reem Alshahrani, Taif University, Saudi Arabia
Mohammed Al-Sarem, Taibah University, Saudi Arabia
Sarah Al-Shareeda, University of Bahrain, Bahrain
Mourad Amad, Bouira University, Algeria
Muhammad Sohaib Ayub, Lahore University of Management Sciences (LUMS), Pakistan
V. Balasubramanian, Arizona State University, USA
Ilija Basicevic, University of Novi Sad, Serbia
Mohamed Benmohammed, University Constantine2, Algeria
Robert Bestak, Czech Technical University in Prague, Czech Republic
Muhammad Danial Bin Zakaria, Universiti Sultan Zainal Abidin, Malaysia
Eugen Borcoci, University "Politehnica"of Bucharest (UPB), Romania
Christos Bouras, University of Patras, Greece

Yimeng Zhao, Facebook, USA
Gaoqiang Zhuo, Castlight Health, USA

Copyright Information

For your reference, this is the text governing the copyright release for material published by IARIA.

The copyright release is a transfer of publication rights, which allows IARIA and its partners to drive the dissemination of the published material. This allows IARIA to give articles increased visibility via distribution, inclusion in libraries, and arrangements for submission to indexes.

I, the undersigned, declare that the article is original, and that I represent the authors of this article in the copyright release matters. If this work has been done as work-for-hire, I have obtained all necessary clearances to execute a copyright release. I hereby irrevocably transfer exclusive copyright for this material to IARIA. I give IARIA permission or reproduce the work in any media format such as, but not limited to, print, digital, or electronic. I give IARIA permission to distribute the materials without restriction to any institutions or individuals. I give IARIA permission to submit the work for inclusion in article repositories as IARIA sees fit.

I, the undersigned, declare that to the best of my knowledge, the article is does not contain libelous or otherwise unlawful contents or invading the right of privacy or infringing on a proprietary right.

Following the copyright release, any circulated version of the article must bear the copyright notice and any header and footer information that IARIA applies to the published article.

IARIA grants royalty-free permission to the authors to disseminate the work, under the above provisions, for any academic, commercial, or industrial use. IARIA grants royalty-free permission to any individuals or institutions to make the article available electronically, online, or in print.

IARIA acknowledges that rights to any algorithm, process, procedure, apparatus, or articles of manufacture remain with the authors and their employers.

I, the undersigned, understand that IARIA will not be liable, in contract, tort (including, without limitation, negligence), pre-contract or other representations (other than fraudulent misrepresentations) or otherwise in connection with the publication of my work.

Exception to the above is made for work-for-hire performed while employed by the government. In that case, copyright to the material remains with the said government. The rightful owners (authors and government entity) grant unlimited and unrestricted permission to IARIA, IARIA's contractors, and IARIA's partners to further distribute the work.

Table of Contents

Power Control based Fair Coexistence of LBT-Free 5G New Radio Small Cells with WiGig Networks

Rony Kumer Saha
Radio and Spectrum Laboratory
KDDI Research, Inc.
2-1-15 Ohara, Fujimino-shi, Saitama, Japan
email: ro-saha@kddi-research.jp

***Abstract*—In this paper, we present a power control technique to coexist in-building small cells of the Fifth-Generation (5G) New Radio (NR) in the 60 GHz band with the incumbent Access Points (APs) of the IEEE 802.11ad/ay standard, also termed as Wireless Gigabit (WiGig). Small cells are not Listen-Before-Talk (LBT) feature enabled. Moreover, each small cell is equipped with a dual-transceiver, one operating in the 28 GHz band exclusively while the other in the 60 GHz band opportunistically. The proposed technique allows each small cell to operate in the 60 GHz band only to serve its downlink traffic by switching its transmission power either to zero or to a minimum allowable level. The minimum power level results in the interference experienced by a WiGig AP (WiAP) that does not exceed its prior interference threshold level set by the WiGig operator to ensure its fairness while coexisting with a small cell. We derive average capacity, Spectral Efficiency (SE), and Energy Efficiency (EE) metrics for NR small cells. With system-level simulation results, it is shown that the proposed technique improves all these above metrics of small cells considerably while ensuring a fair coexistence of small cells with incumbent WiAPs by limiting the interference at a WiAP to the maximum allowable level (i.e., the interference threshold level).**

Keywords—5G; millimeter-wave; unlicensed band; new radio; small cell; IEEE 802.11 ad/ay; power control.

I. INTRODUCTION

The continuing growth in mobile devices and data traffic over the past decade causes mobile network operators (MNOs) to face tremendous challenges since the availability of the mobile spectrum for an MNO has not been increased correspondingly. Though several approaches, such as small cell deployments have been employed, no significant improvement toward addressing the growing demand to serve data traffic has been observed. This causes the focus of an MNO to shift from serving its data traffic by the allocated licensed spectrum only to the unlicensed spectrum bands as well. Globally, a large amount of spectrum is available in the unlicensed bands, including 2.4 GHz, 5 GHz, and 60 GHz. A major feature of the unlicensed bands is the ability of a user to get access freely to them. However, because of the presence of the incumbent WiFi networks in the unlicensed bands, proper co-channel interference (CCI) management is necessary to coexist a cellular network with a WiFi network in the same unlicensed band.

In this regard, by enabling cellular nodes (e.g., small cells) with Listen-Before-Talk (LBT) (Alhulayil and Lopez-Benitez, [1]), a fair coexistence of cellular and WiFi nodes can be made possible. The LBT is basically similar to the Carrier-Sense Multiple Access with Collision Avoidance (CSMA/CA). Instead of allowing a cellular node to always use a channel, it shares between a cellular node and a WiFi Access Point (AP) fairly (Zhang et al. [2]) by periodically stopping the cellular node to occupy the channel and detecting the activities of other shared nodes on the channel. Several studies also showed that the LBT is critical for a fair coexistence between a cellular network such as Long-Term Evolution (LTE) and a Wi-Fi network (Kwan et al. [3], Chaves et al. [4]). However, LBT is not used in all regions such as the United States of America (USA) and China where LBT is not required particularly for early commercialization (Lagen et al. [5]). Hence, cellular nodes are enabled with LBT, they do not have sensing capabilities such as the CSMA/CA protocol of WiFi networks to avoid a collision. In this regard, the coexistence of small cells can be provided by managing CCI with WiFi networks in time and power domains.

In this direction, numerous studies already addressed the coexistence issues between cellular and WiFi networks in the time-domain using the Almost Blank Subframe (ABS) based Enhanced Intercell Interference Coordination (eICIC) technique in LTE. For example, by employing ABSs, Almeida et al. [6] proposed a scheme to coexist LTE with WiFi in an unlicensed band. Likewise, Nihtilä et al. [7] proposed the LTE muting mechanism to allow access to the channel to WiFi users and Zhang et al. [8] presented an ABS-based coexistence scheme to avoid co-channel interference between small cells and WiFi systems.

With regard to providing the coexistence between cellular and WiFi networks in the power-domain, Huang et al. [9] discussed the coexistence of LTE/WiFi in the power domain such that by adjusting the output power of LTE nodes, the transmission opportunity of WiFi nodes can be changed. Sagari et al. [10] proposed Wi-Fi and LTE coordination algorithms based on optimization in the power and frequency domain. Further, Chaves et al. in [4] proposed to use the uplink power control to improve the performance of coexistence of LTE with WiFi by introducing an additional factor to the conventional uplink power control mechanism of LTE. Besides, Hang et al. [11] proposed a Power Control-based Spatial Reuse scheme to increase the probability of simultaneous transmissions of Licensed-Assisted Access (LAA) and WiFi. Moreover, in [12], Xia et al. studied the use of transmit power control, as well as clear channel assessment, mechanisms in unlicensed LTE systems by considering that all stations use the same fixed transmit power.

However, different from these above contributions in power-domain, in this paper, we present a simple, yet effective, transmit power control technique for in-building small cells of

 ISBN: 978-1-61208-895-2

Fifth-Generation (5G) New Radio (NR) to coexist with the incumbent WiFi Access Points (WiAPs) of the Wireless Gigabit (WiGig) in the 60 GHz band. In doing so, we first present the system architecture and the coexistence mechanism in Section II, followed by the mathematical analysis to derive average capacity, Spectral Efficiency (SE), and Energy Efficiency (EE) metrics for NR small cells in Section III. We evaluate the performance of the proposed technique in Section IV and conclude the paper in Section V.

II. System Architecture and Proposed Coexistence Mechanism

Consider a set of small cells and WiAPs such that one from each set is deployed per apartment of any multistory building located within the coverage of a macrocell of a 5G NR operator. A set of picocells are also located within the macrocell coverage to offload some macrocell traffic. Each small cell or WiAP serves one User Equipment (UE) at a time. For clarity, we consider only one apartment to show the coexistence of a small cell and a WiAP as shown in Figure 1(a). From Figure 1(a), it can be found that each small cell is equipped with two transceivers, one operates in the 28 GHz band and the other in the 60 GHz band.

Since the 28 GHz band is a licensed band for an MNO, the transceiver operating at the 28 GHz band can serve both the uplink and downlink traffic at all time. However, since WiAPs operate in the 60 GHz band by default, and small cells are not Listen-Before-Talk (LBT) enabled, it can be possible that all WiAPs are blocked by the small cells due to having relatively a higher interference margin of a small cell than that of a WiAP. Hence, to overcome this problem, we propose the following power control technique to coexist small cells with WiAPs as shown in Figure 2(b).

Small cells of any 5G NR can get access to the 60 GHz band either when no UEs of any WiGig network are present within an apartment of a multistory building or when small cells of any 5G NR can operate in the 60 GHz band at a reduced transmission power causing less interference than that of the interference threshold set by the corresponding WiGig network, as shown in Figure 1(b).

The presence of a UE of a small cell can be sensed by the WiAP by detecting and measuring the 60 GHz channel energy, whereas the transmission of a WiAP can be identified either by the small cell using its transceiver operating at the 28 GHz or by the UE of the small cell in the uplink at the 28 GHz band. Note that the WiAP stops the transmission due to its inherent CSMA/CA protocol to avoid collision with the small cell. An example of opportunistic subframe allocation to small cells to coexist with WiAPs in the 60 GHz spectrum band by employing the proposed power control technique is shown in Figure 1(c) and is described in the following.

A subframe in the 60 GHz is allocated to either a small cell or a WiAP depend on the presence of their UEs at any time, as well as the level of interference experienced by the UE of the WiAP as compared to that of its threshold interference. More specifically, given that a UE of the small cell is present in an apartment, a subframe is allocated to a small cell only under the following conditions:

- when no UEs of the WiAP is present.
- when a UE of the WiAP is present, and the interference experienced by the WiAP UE is above the threshold interference.

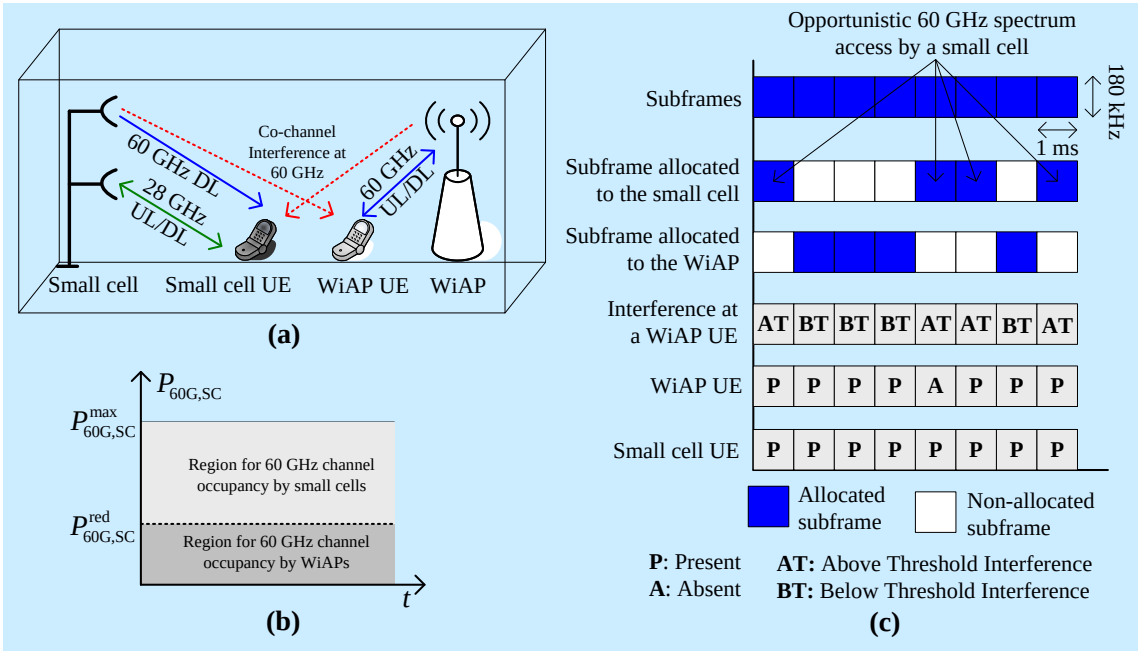

Figure 1. (a) Coexistence of a small cell and a WiAP in an apartment of a building. (b) Small cell transmission power control technique. (c) An example of opportunistic 60 GHz spectrum access by a small for a number of subframes.

 ISBN: 978-1-61208-895-2

However, if the interference experienced by the UE of the WiAP is below the threshold interference in a subframe, no collision can be detected by the CSMA/CA protocol of the WiAP, and hence, the corresponding subframe is allocated to the WiAP.

III. MATHEMATICAL ANALYSIS

Let S_{M}, S_{P}, and S_{F} denote, respectively, the number of macrocells of a 5G NR MNO, the number of picocells per macrocell, and the number of small cells in a building. Let $M_{2\mathrm{G}}$, $M_{28\mathrm{G}}$, and $M_{60\mathrm{G}}$ denote, respectively, the number of Resource Blocks (RBs) of 2 GHz, 28 GHz, and 60 GHz spectra where an RB is equal to 180 kHz. Also, let $\boldsymbol{T}$ denote the simulation run time with the maximum time of Q (in time step each lasting 1 ms) such that $\boldsymbol{T}$= {1, 2, 3,…,Q}. Following [13], the arrival process of UEs of a 5G NR small cells and WiGig operators can be assumed to follow the Poisson processes with a mean λ_{NR} and λ_{WiG}, respectively, over a certain observation time T. Hence, the amount of time in terms of the number of Transmission Time Intervals (TTIs) that 5G NR small cells and WiAPs in a building serve their corresponding UEs in Q can be expressed, respectively, as follows.

$$T_{\mathrm{NR}} = \left\lceil \left(\frac{\lambda_{\mathrm{NR}}}{(\lambda_{\mathrm{NR}} + \lambda_{\mathrm{WiG}})} \right) \times Q \right\rceil \tag{1}$$

Let P_{MC} and P_{PC} denote, respectively, the transmission power of a macrocell and a picocell. Let $I^{\mathrm{th}}_{60\mathrm{G,WiG}}$ denote the threshold interference value for a WiAP. Also, let $P^{\max}_{60\mathrm{G,SC}}$ and $P^{\mathrm{red}}_{60\mathrm{G,SC}}$ denote, respectively, the maximum transmission power and the reduced transmission power of a small cell when operating in the 60 GHz band. Let $I_{60\mathrm{G,SC}}$ denote the interference experienced by a WiAP due to $P^{\mathrm{red}}_{60\mathrm{G,SC}}$ such that $I_{60\mathrm{G,SC}} \le I^{\mathrm{th}}_{60\mathrm{G,WiG}}$. Hence, the transmission power of a small cell when operating at 60 GHz can be expressed as follows.

$$P_{60\mathrm{G,SC}} = \begin{cases} P^{\max}_{60\mathrm{G,SC}}, & \text{if } I_{60\mathrm{G,SC}} = 0 \\ P^{\mathrm{red}}_{60\mathrm{G,SC}}, & \text{if } I_{60\mathrm{G,SC}} \neq 0 \end{cases} \tag{2}$$

Now the received Signal-to-Interference-Plus-Noise Ratio (SINR) at RB=i in TTI=t at a UE of a small cell is given by

$$\rho_{t,i} = \left(\frac{P_{t,i}}{(N^{\mathrm{s}}_{t,i} + I_{t,i})} \right) \times H_{t,i} \tag{3}$$

where $P_{t,i}$, $N^{\mathrm{s}}_{t,i}$, $I_{t,i}$, and $H_{t,i}$ denote, respectively, transmission power, noise power, interference power, and link loss at RB=i in TTI=t.

Using Shannon's capacity formula, a link throughput at RB=i in TTI=t for an MNO o in bps per Hz is given by [14]

$$\sigma_{t,i}(\rho_{t,i}) = \begin{Bmatrix} 0, & \rho_{t,i} < -10\,\mathrm{dB} \\ \beta \log_2\left(1 + 10^{(\rho_{t,i}(\mathrm{dB})/10)}\right), & -10\,\mathrm{dB} \le \rho_{t,i} \le 22\,\mathrm{dB} \\ 4.4, & \rho_{t,i} > 22\,\mathrm{dB} \end{Bmatrix} \tag{4}$$

where β denotes the implementation loss factor.

The average capacity of all macrocell UEs of a 5G NR can be given by

$$\sigma_{2\mathrm{G}} = \sum_{t=1}^{Q} \sum_{i=1}^{M_{2\mathrm{G}}} \sigma_{t,i}(\rho_{t,i}) \tag{5}$$

where σ and ρ are responses over $M_{2\mathrm{G}}$ RBs of all macro UEs in $t \in \boldsymbol{T}$.

Now, the average capacity served by transceiver 1 of all small cells in the building is given by,

$$\sigma^{\mathrm{Tr\,1}}_{28\mathrm{G}} = \sum_{s=1}^{S_{\mathrm{F}}} \sum_{t \in \boldsymbol{T}} \sum_{i=1}^{M_{28\mathrm{G}}} \sigma_{s,t,i}(\rho_{s,t,i}) \tag{6}$$

Similarly, the average capacity served by transceiver 2 of all small cells in the building is given by,

$$\sigma^{\mathrm{Tr\,2}}_{60\mathrm{G}} = \sum_{s=1}^{S_{\mathrm{F}}} \sum_{t \in \boldsymbol{T}_{\mathbf{NR}}} \sum_{i=1}^{M_{60\mathrm{G}}} \sigma_{s,t,i}(\rho_{s,t,i}) \tag{7}$$

So, the total average capacity served by both transceivers of all small cells in the building is given by,

$$\sigma^{\mathrm{Tr\,1+Tr\,2}}_{\mathrm{Dual\,Band}} = \sigma^{\mathrm{Tr\,1}}_{28\mathrm{G}} + \sigma^{\mathrm{Tr\,2}}_{60\mathrm{G}} \tag{8}$$

Due to small coverage, low transmission power, and high distance-dependent path loss, we assume similar indoor signal propagation characteristics for both 28 GHz and 60 GHz. Hence, by linear approximation, the system-level average capacity, SE, and EE, respectively, for all small cells of a 5G NR is given by,

$$\sigma^{\mathrm{5G\,NR}}_{\mathrm{Sys}} = \sigma_{2\mathrm{G}} + \sigma^{\mathrm{Tr\,1+Tr\,2}}_{\mathrm{Dual\,Band}} \tag{9}$$

$$\gamma^{\mathrm{5G\,NR}}_{\mathrm{Sys}} = \frac{\sigma^{\mathrm{5G\,NR}}_{\mathrm{Sys}}}{\left((M_{2\mathrm{G}} + M_{28\mathrm{G}}) \times Q\right)} \tag{10}$$

$$\varepsilon^{\mathrm{5G\,NR}}_{\mathrm{Sys}} = \frac{\left(\left(\begin{pmatrix} \left(L \times S_{\mathrm{F}} \times \left(P_{28\mathrm{G,SC}} + P_{60\mathrm{G,SC}}\right)\right) + \\ \left(S_{\mathrm{P}} \times P_{\mathrm{PC}}\right) + \left(S_{\mathrm{M}} \times P_{\mathrm{MC}}\right) \end{pmatrix} \times Q \right) \right)}{\sigma^{\mathrm{5G\,NR}}_{\mathrm{Sys}}} \tag{11}$$

Note that for the SE estimation in (10), only the licensed spectra are considered since licensed spectra are not free of cost and each operator needs to pay for the spectrum licensing fee.

IV. PERFORMANCE EVALUATION AND COMPARISON

Table I shows the simulation parameters and assumptions used to evaluate the performances of the proposed technique. Figure 2 shows SE and EE responses of small cells in a building

due to the variation in the interference threshold $I^{th}_{60G,WiG}$ at a WiAP. As the interference threshold requirement increases, i.e. the value of $I^{th}_{60G,WiG}$ decreases, both SE and EE performances of small cells of 5G NR improve nonlinearly. This is because, with an increase in $I^{th}_{60G,WiG}$, small cells can increase the transmission power in the 60 GHz band, resulting in improving the capacity logarithmically following (4). This, however, causes a corresponding reduction in the capacity, and hence the SE and EE performances of WiAPs. Moreover, using (7), an increase in the transmission time T_{NR} of small cells increases the overall capacity, and hence the SE and EE of small cells. In summary, T_{NR} and $I^{th}_{60G,WiG}$ play considerable role in trading-off the coexistence performances, in terms of the average capacity, SE, and EE, of both small cells of a 5G NR network and WiAPs of a WiGig network.

TABLE I
SIMULATION PARAMETERS AND ASSUMPTIONS

Parameters and Assumptions			Value
Number of 5G NR-U and WiGig operators, respectively			1, 1
Spectrum bandwidth of NR	2 GHz (Non-LOS), 28 GHz (LOS), and 60 GHz (LOS), respectively		10 MHz, 50 MHz, and 100 MHz
Number of cells	Macrocells, picocells, and small cells		1, 2, and 9
Interference threshold, $I^{th}_{60G,WiG}$			10%, 15%, and 20% of $P^{max}_{60G,SC}$
Cellular layout[2], inter-site distance (ISD)[1,2], transmission direction			Hexagonal grid, dense urban, 3 sectors per macrocell site, 1732 m, downlink
Total base station transmit power (dBm)		Macrocell[1] and picocell[1]	46 and 37
		Small cell operating in 28 GHz[1]	19
		Small cell operating in 60 GHz[1]	17.3
Co-channel small-scale fading model[1]		2 GHz	Frequency selective Rayleigh
		28 GHz	no small-scale fading effect
		60 GHz	no small-scale fading effect
Path loss	MBS and a UE[1]	Outdoor macrocell UE	PL(dB)=15.3 + 37.6 $\log_{10}R$, R is in m
		Indoor macrocell UE	PL(dB)=15.3 + 37.6 $\log_{10}R$ + L_{ow}, R is in m and L_{ow}=20 dB
	PBS and a UE[1]		PL(dB)=140.7+36.7 $\log_{10}R$, R is in km
	SBS and a UE[1,2]	28 GHz	PL(dB)=61.38+17.97 $\log_{10}R$, R is in m
		60 GHz	PL(dB)=68+21.7$\log_{10}(R)$, R in m
Lognormal shadowing standard deviation (dB)		MBS[2] and PBS[1]	8 and 10
		SBS in 28 GHz and 60 GHz[2]	9.9 and 0.88
Antenna configuration			Single-input single-output for all BSs and UEs
Antenna pattern (horizontal)			Directional (120^0) for MBS[1], omnidirectional for PBS[1] and SBS[1]
Antenna gain plus connector loss (dBi)		MBS[2] , PBS[1], and SBS[1]	14, 5, and 5
UE antenna gain[2]	2 GHz, 28 GHz, and 60 GHz (Biconical horn)		0 dBi, 5 dBi, and 5 dBi
UE noise figure[2] , UE speed[1], and indoor macrocell UE[1]			9 dB (for 2 GHz) and 10 dB (for 28 GHz and 60 GHz), 3 km/hr, and 35%
Picocell coverage[1], the total number of macrocell UEs, and macrocell UEs offloaded to all picocells[1]			40 m (radius), 30, 2/15
3D multistory building and SBS models (square-grid apartments)		Number of buildings	1
		Number of floors per building	1
		Number of apartments per floor	9
		Number of SBSs per apartment	1
		Area of an apartment	10×10 m^2
Scheduler and traffic model[2]			Proportional Fair and full buffer
Type of SBSs			Closed Subscriber Group femtocell BSs
TTI[1], FPP, and PF scheduler time constant (t_c)			1 ms, 8 ms, and 100 ms
Total simulation run time			8 ms

taken [1]from [15], [2]from [16].

 ISBN: 978-1-61208-895-2

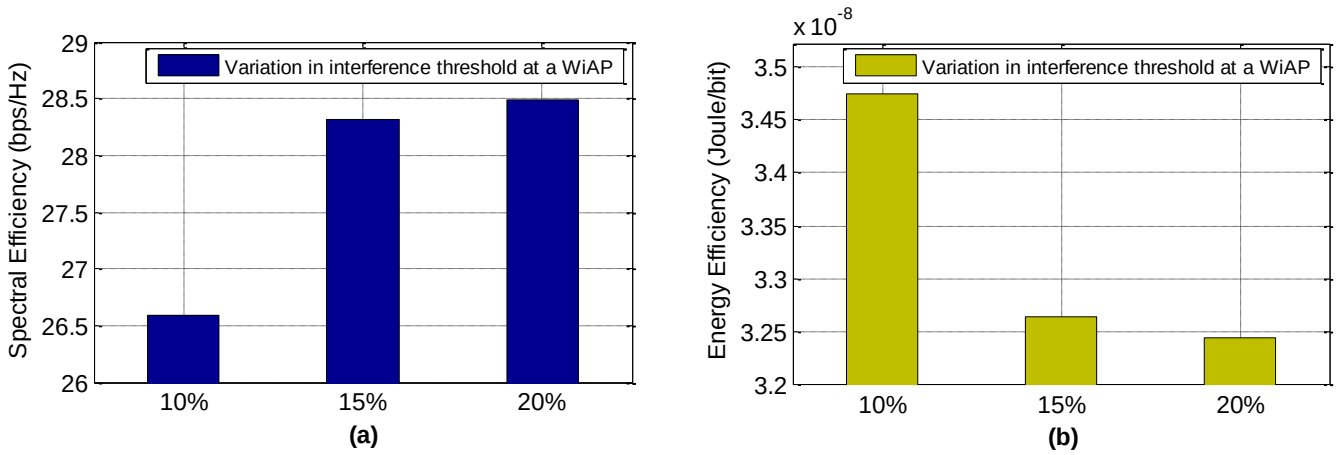

Figure 2. SE and EE responses of 5G NR small cells due to the variation in the interference threshold in the percentage of $P_{60G,SC}^{max}$ at a WiAP.

With regards to the other existing techniques, the proposed technique benefits from the fact that it does not impact the air interface protocol of cellular systems, as well as can meet the global regulations. Moreover, this technique is typically used together with other coexistence techniques. However, it is less fair to resource allocations than other techniques and is typically interference measurement based [17].

V. CONCLUSION

In this paper, we have presented a transmission power control technique for LBT-free 5G NR small cells to coexist with WiAPs in the 60 GHz band within a building. With system-level simulation results, it has been shown that the proposed technique can improve the average capacity, SE, and EE of small cells of a 5G NR while ensuring fair coexistence with WiAPs by maintaining a maximum interference level at a WiAP limited to its interference threshold. More specifically, an increase in the interference threshold of WiAPs results in a nonlinear increase in the SE and EE of small cells while decreasing the SE and EE of WiAPs. However, an increase in the transmission time of either small cells or WiAPs causes a corresponding linear increase in the SE and EE. Hence, the transmission time and the interference threshold of WiAPs play noticeable roles in trading-off the coexistence performances of small cells of a 5G NR and WiAPs of a WiGig.

REFERENCES

[1] M. Alhulayil and M. Lopez-Benitez, "Coexistence Mechanisms for LTE and Wi-Fi Networks Over Unlicensed Frequency Bands," Proc. 2018 11th International Symposium on Communication Systems, Networks & Digital Signal Processing (CSNDSP), Budapest, Hungary, 2018, pp. 1-6, doi: 10.1109/CSNDSP.2018.8471826.

[2] R. Zhang et al., "LTE-Unlicensed: The Future of Spectrum Aggregation for Cellular Networks," IEEE Wireless Communications, vol. 22, no. 3, pp. 150-159, June 2015, doi: 10.1109/MWC.2015.7143339.

[3] R. Kwan, et al., "Fair Co-Existence of Licensed Assisted Access LTE (LAA-LTE) and Wi-Fi in Unlicensed Spectrum," Proc. 2015 7th Computer Science and Electronic Engineering Conference (CEEC), pp. 13-18, 2015.

[4] F. S. Chaves et al., "LTE UL Power Control for the Improvement of LTE/Wi-Fi Coexistence," Proc. 2013 IEEE 78th Vehicular Technology Conference (VTC Fall), Las Vegas, NV, USA, 2013, pp. 1-6, doi: 10.1109/VTCFall.2013.6692275.

[5] S. Lagen et al., "New Radio Beam-Based Access to Unlicensed Spectrum: Design Challenges and Solutions," Proc. IEEE Communications Surveys & Tutorials, vol. 22, no. 1, pp. 8-37, Firstquarter 2020, doi: 10.1109/COMST.2019.2949145.

[6] E. Almeida et al., "Enabling LTE/WiFi coexistence by LTE blank subframe allocation," Proc. 2013 IEEE International Conference on Communications (ICC), Budapest, 2013, pp. 5083-5088, doi: 10.1109/ICC.2013.6655388.

[7] T. Nihtilä et al., "System Performance of LTE and IEEE 802.11 coexisting on a Shared Frequency Band," Proc. 2013 IEEE Wireless Communications and Networking Conference (WCNC), Shanghai, 2013, pp. 1038-1043, doi: 10.1109/WCNC.2013.6554707.

[8] H. Zhang, X. Chu, W. Guo, and S. Wang, "Coexistence of Wi-Fi and Heterogeneous Small Cell Networks Sharing Unlicensed Spectrum," IEEE Commun. Mag., vol. 53, no. 3, pp. 158-164, March 2015, doi: 10.1109/MCOM.2015.7060498.

[9] Y. Huang, Y. Chen, Y. T. Hou, W. Lou, and J. H. Reed, "Recent Advances of LTE/WiFi Coexistence in Unlicensed Spectrum," IEEE Network, vol. 32, no. 2, pp. 107-113, March-April 2018, doi: 10.1109/MNET.2017.1700124.

[10] S. Sagari, S. Baysting, D. Saha, I. Seskar, W. Trappe and D. Raychaudhuri, "Coordinated Dynamic Spectrum Management of LTE-U and Wi-Fi Networks," Proc. 2015 IEEE International Symposium on Dynamic Spectrum Access Networks (DySPAN), Stockholm, Sweden, 2015, pp. 209-220, doi: 10.1109/DySPAN.2015.7343904.

[11] D. Hang, M. Yang, Z. Yan, and B. Li, "Power Control Based Spatial Reuse for LAA and WiFi Coexistence." In: Lin YB., Deng DJ. (eds) Smart Grid and Internet of Things. SGIoT 2020. Lecture Notes of the Institute for Computer Sciences, Social Informatics and Telecommunications Engineering, vol 354. Springer, Cham., pp. 363-384, doi.org/10.1007/978-3-030-69514-9_29

[12] P. Xia, Z. Teng, and J. Wu, "How Loud to Talk and How Hard to Listen-Before-Talk in Unlicensed LTE," Proc. 2015 IEEE International Conference on Communication Workshop (ICCW), London, UK, 2015, pp. 2314-2319, doi: 10.1109/ICCW.2015.7247526.

 ISBN: 978-1-61208-895-2

[13] J. D. Chimeh, M. Hakkak, and S. A. Alavian, “Internet Traffic and Capacity Evaluation in UMTS Downlink,” Proc. FGCN, December 2007, pp. 547-552.

[14] R. K. Saha “Spectrum Allocation and Reuse in 5G New Radio on Licensed and Unlicensed Millimeter-Wave Bands in Indoor Environments,” Mobile Information Systems Journal, vol. 2021, art. ID 5538820, pages 21, 2021. doi: 10.1155/2021/5538820

[15] Evolved Universal Terrestrial Radio Access (E-Utra); Radio Frequency (rf) System Scenarios. Document 3GPP TR 36.942, V.1.2.0, 3rd Generation Partnership Project, Jul. 2007. Available online: https://portal.3gpp.org/ desktopmodules /Specifications/ Specification Details.aspx?specificationId=2592 [retrived: February, 2021].

[16] Simulation Assumptions and Parameters For FDD HeNB RF Requirements. document TSG RAN WG4 (Radio) Meeting #51, R4-092042, 3GPP, May 2009. [retrived: February, 2021].

[17] Y. Huang, Y. Chen, Y. T. Hou, W. Lou, and J. H. Reed, “Recent Advances of LTE/WiFi Coexistence in Unlicensed Spectrum,” *IEEE Netw.*, vol. 32, no. 2, pp. 107-113, March-April 2018

 ISBN: 978-1-61208-895-2

Unlicensed Spectrum Bands for Cellular Mobile Networks-An Overview

Rony Kumer Saha
Radio and Spectrum Laboratory
KDDI Research, Inc.
2-1-15 Ohara, Fujimino-shi, Saitama 356-8502, Japan
email: ro-saha@kddi-research.jp

***Abstract*—This paper provides a survey on the available unlicensed spectrum bands for cellular mobile networks. Unlicensed spectrum bands in both the sub-7 GHz, including 2.4 GHz, 5 GHz, and 6 GHz, as well as millimeter-wave, including 60 GHz, for the current and future mobile networks, are discussed. Major aspects of each unlicensed band, notably operational region, regulatory requirement, existing technology, available bandwidth, spectrum range, benefit, and challenge are surveyed. A comparative framework, including these above aspects, is then developed in a tabular form to find an appropriate unlicensed spectrum band corresponding to each aspect. Finally, we point out the major benefits and challenges of operating cellular mobile networks on unlicensed bands.**

Keywords-Unlicensed band; survey; cellular network; millimeter-wave.

I. INTRODUCTION

Radio spectrum is limited and not allocated to a Mobile Network Operator (MNO) in proportionate with its traffic demand [1]. To address the scarcity of the available licensed spectrum, techniques, including cell splitting and small cell deployment, have been proposed [2]. However, due to employing such techniques, no noticeable impact has been observed, which causes the focus of MNOs to shift from the licensed-only spectrum to the unlicensed spectrum. Recently, the operations of the Third Generation Partnership Project (3GPP)-based cellular technologies in the unlicensed bands have been introduced.

Cellular technologies may operate in one or more unlicensed spectrum bands, including 2.4 GHz, 5 GHz, 6 GHz, and 60 GHz. Because the operation of the unlicensed spectrum is marked by regional regulatory authorities [3], of these, 2.4 GHz, 5 GHz, and 60 GHz bands are available worldwide [4], whereas the 6 GHz band is currently available in Europe and the USA. In addition to these above-unlicensed bands, cellular technologies, particularly, Fifth-Generation (5G) New Radio Unlicensed (NR-U) can also use shared bands, including 3.5 GHz and 37 GHz, only in the USA [5]. Due to not having a significant difference in signal propagations, according to the 3GPP, 2.4 GHz, 3.5 GHz, 5 GHz, and 6 GHz are classified as low-frequency bands below 7 GHz, whereas 37 GHz and 60 GHz high-frequency bands are classified as millimeter-wave (mmWave) bands. These two unlicensed frequency ranges are targeted for 5G NR-U operations [6].

Typically, an unlicensed spectrum is used by the Institute of Electrical and Electronics Engineers (IEEE) 802.11, also termed as Wireless Fidelity (WiFi) [7], technologies in addition to Bluetooth and ZigBee. Hence, to operate cellular technologies in the same unlicensed band at the same place simultaneously, a proper coexistence mechanism to manage Co-Channel Interference (CCI) between cellular and WiFi technologies is necessary. Coexistence mechanisms can be developed in two ways depending on whether or not modifications on the existing cellular networks are employed. If modifications are employed, a cellular network is enabled with a carrier sensing mechanism, termed as Listen-Before-Talk (LBT).

LBT is a contention-based medium access technique that shares a channel between a cellular node and a WiFi Access Point (AP) fairly [8] by enabling a cellular node to stop periodically its channel occupancy to help avoid CCI due to the coexistence with the WiFi AP. Likewise, numerous coexistence mechanisms without employing LBT have been proposed to manage CCI such as channel selection, carrier sense adaptive transmission, fully blank subframe, and transmit power control. In channel selection, a cellular node measures the level of interference on each channel by detecting the channel's energy so that the data transmission can be made over a channel with the minimum level of interference. In carrier sense adaptive transmission, by dividing time into cycles each consisting of an on period and an off period such that a cellular node can transmit data during the on-state of a cycle. Likewise, in the fully blank subframe, time is segmented into transmission time intervals (TTIs) such that a cellular node can use a set of TTIs over a certain period T, whereas, IEEE 802.11 standards can transmit using the remaining number of TTIs in T orthogonally to each other in time. A key feature of each of these mechanisms is that none requires modifications on existing cellular networks. Since our focus is mainly on the unlicensed bands for cellular networks, a detailed discussion on coexistence mechanisms is out of the scope of this paper.

Numerous existing works addressed the operation of cellular standards such as Long-Term Evolution Unlicensed (LTE-U), Licensed Assisted Access (LAA), and NR-U on unlicensed bands from specific viewpoints, including coexistence mechanisms [9]-[19], unlicensed bands (e.g., 5

 ISBN: 978-1-61208-895-2

GHz [20]-[22], 6 GHz [23], and 60 GHz [24]), coexistence studies [25]-[26] and scenarios [27], fairness conditions [28]-[29], standardization efforts [30], challenges, and open problems [3] [31]. Different from these above existing studies, in this paper, we provide a survey on unlicensed spectrum bands from a nonspecific viewpoint that takes into account all available unlicensed spectrum bands in both the sub-7 GHz, including 2.4 GHz, 5 GHz, and 6 GHz, as well as mmWave, including 60 GHz, for the cellular networks. Major aspects of each unlicensed band, including operational region, regulatory requirement, existing technology, available bandwidth, spectrum range, benefit, and challenge, are discussed. A comparative framework of all these aspects is then developed, and major benefits and challenges regarding the operation of cellular networks on unlicensed bands are pointed out.

The paper is organized as follows. In Section II, an overview of unlicensed spectrum bands, including 2.4 GHz, 5 GHz, 6 GHz, and 60 GHz, for cellular networks, as well as a comparative framework for a number of major aspects among these unlicensed bands are given. In Section III, the operation of cellular technologies, including LTE-U, LAA, and NR-U, in unlicensed bands is discussed. Key benefits and challenges of operating cellular networks in the unlicensed band are identified in Section IV. We conclude the paper in Section V. A list of abbreviations is given in Appendix I.

II. Overview of Unlicensed Spectrum Bands for Cellular Technologies

A. 2.4 GHz Unlicensed Band

The 2.4 GHz band is the first unlicensed band released by the Federal Communications Commission (FCC) for commercial use and is currently the most utilized unlicensed shared band [8]. In the 2.4 GHz band, the bandwidth is divided into 14 channels with a separation of 5 MHz from one channel to another. In the USA, operations on channels 12 and 13 are allowed only under low power conditions [32]. Likewise, in Canada, of a total of 12 channels (from channel 1 to channel 12) available to use, the operation on channel 12 is limited by the transmission power. However, most of the rest of the world can use 13 channels (from channel 1 to channel 13) [32], and channel 14 is available only in Japan.

B. 5 GHz Unlicensed Band

The use of the 5 GHz band depends on its requirement in a country [20]. The 5.15-5.35 GHz band is available in the USA, China, South Korea, Europe, Japan, and India; the 5.47-5.725 GHz is available in the USA, South Korea, Europe, and Japan; and the 5.725-5.85 GHz is available in the USA, China, South Korea, and India [7]. Additionally, the 5.35-5.47 GHz and the 5.85-5.925 GHz unlicensed spectra are being considered to make available in the USA and Canada [3] [7] [8]. Moreover, European Commission (EC) also recently proposed to use the 5.725-5.85 GHz spectrum band [8]. In general, due to the clearer channel condition, wider spectrum, and easier implementation [8], the 5 GHz band is considered favorable to other unlicensed bands.

C. 6 GHz Unlicensed Band

The 6 GHz spectrum band is available from 5.925 to 6.425 GHz in Europe, whereas from 5.925 to 7.125 GHz in the USA [23]. Recently, 5.925-6.425 GHz [33] spectrum and 5.925 GHz-7.125 GHz spectrum have been proposed, respectively, by the EC and the FCC under part 15 rules for the unlicensed access [34]-[35]. Hence, the amount of the unlicensed spectrum available in Europe is 500 MHz and in the USA is 1200 MHz, which can help address the high capacity demand of future mobile networks. Since much of the 6 GHz band is occupied by some licensed services, such as microwave links, fixed satellite systems, and mobile services, Automatic Frequency Coordination (AFC) is needed by unlicensed users to protect licensed services. Unlicensed users are also required to control the transmit power and restrict their coverage to indoors [6].

D. 60 GHz Unlicensed Band

The 60 GHz band is considered for the NR-U to provide directional communications using beamforming to overcome propagation constraints [36]-[37]. Due to operating Wireless Gigabit (WiGig) in the 60 GHz band, the NR-U standard needs to coexist fairly with the WiGig standard. The 60 GHz band ranges from 57 GHz to 71 GHz [38]. The bandwidth available in the unlicensed 60 GHz band is more than that of the aggregate bandwidth of all the other unlicensed bands [39]. The minimum available bandwidth in a region is more than 3 GHz, and at least 7 GHz of bandwidth can be used in most regions in the 60 GHz band in comparison with just about 500 MHz of usable bandwidth in the 5 GHz band and less than 85 MHz of bandwidth in the 2.4 GHz band in most regions [39]. Due to this reason, the 60 GHz band is suited for serving high data rate demand in magnitudes of Gbps over short distances.

III. Cellular Technologies in the Unlicensed Spectrum Bands

Long-Term Evolution (LTE) is the first cellular-based technology extended with a view to operating in the sub-7 GHz unlicensed spectrum bands in 2015, whereas NR-U is the first cellular-based technology that includes operations in the mmWave unlicensed bands [4]-[5]. Hence, since cellular technologies in the previous generations, i.e., Fourth-Generation (4G) LTE, were not allowed to use mmWave bands, two standards of LTE working in the unlicensed bands, namely LTE-U and LAA, operate in the 5 GHz band. However, unlike LTE that operates only in the 5 GHz unlicensed spectrum, NR-U can operate on multiple spectrum bands, including mmWave bands, e.g., sub-7 GHz and 60 GHz [4]. Moreover, like LTE, there are a number of

 ISBN: 978-1-61208-895-2

variants of 5G NR-U, including 5G NR-U Standalone operating only in an unlicensed spectrum band (e.g., 60 GHz) and 5G NR-U Anchored operating in both the licensed spectrum and the 60 GHz unlicensed spectrum. On the other hand, MulteFire is developed by the MulteFire Alliance considering a Standalone deployment in the unlicensed bands using an LBT-based channel access scheme [40].

Though existing IEEE and 3GPP-based technologies operate in the unlicensed bands on a competitive basis, such competition results in convergence to use and develop similar features in the radio access in the latest releases and amendments [4], e.g., the use of LBT to 3GPP technologies developed in line with Carrier-Sense Multiple Access with Collision Avoidance (CSMA/CA) inherent to the IEEE 802.11 technologies. Table I shows comparisons in terms of numerous aspects among 2.4 GHz, 5 GHz, 6 GHz, and 60 GHz unlicensed spectrum bands. From Table I, it can be observed that a total of about 2 GHz unlicensed bandwidth is available below 7 GHz for omnidirectional communications at the 2.4 GHz, 5 GHz, and 6 GHz bands [34]. Moreover, a large amount of 9 GHz of spectrum in Europe and 14 GHz unlicensed spectrum in the USA is available in the 60 GHz band for directional communications [41]-[42].

IV. Major Benefits and Challenges from Operating Cellular Networks in the Unlicensed Bands

A. Benefits to Operate in the Unlicensed Bands

By operating cellular networks such as LTE and NR in the unlicensed bands, significant benefits in several aspects can be achieved. A few noticeable benefits are discussed in the following.

1) High capacity, spectral efficiency, and data rates: Employing the Carrier Aggregation (CA) technology, along with the allocated licensed spectrum to an MNO of a cellular network, the unlicensed spectrum can also be used to serve user traffic [8]. Due to the addition of the unlicensed spectrum, the combined spectrum bandwidth of an MNO increases. Moreover, due to the availability of an enormous amount of spectrum bandwidth in the 60 GHz mmWave band, the aggregate bandwidth of an MNO can be increased even further. Since the mmWave spectrum is inherently path loss limited, the 60 GHz unlicensed spectrum is suitable to use within indoor environments. Because the capacity is directly proportional to the available channel bandwidth, the use of the unlicensed spectrum in a cellular network helps increase its overall capacity, spectral efficiency, as well as data rates per user.

2) Data offloading: Given that small cells operate in both the licensed and unlicensed bands, using the CA

TABLE I
A COMPARATIVE FRAMEWORK OF UNLICENSED BANDS FOR CELLULAR TECHNOLOGIES.

Features	Unlicensed spectrum bands			
	2.4 GHz	**5 GHz**	**6 GHz**	**60 GHz**
Classification	Mid-bands (sub-7 GHz)	Mid-bands (sub-7 GHz)	Mid-bands (sub-7 GHz)	High-bands (mmWave)
Availability	Worldwide	Worldwide	Europe and the USA	Worldwide
Regulatory requirement	The maximum data rate, multiple access methods, digital modulation scheme, maximum coverage distance, and media access protocol [43]	The maximum in-band output power, out-of-band and spurious emissions, DFS, LBT, and Transmit Power Control (TPC) [44]	DFS, AFC, TPC, and indoor coverage [6]	Short-range communication, Equivalent Isotropic Radiated Power (EIRP), EIRP densities, maximum power, and antenna gains [45]-[46]
Existing technologies	802.11b/g	802.11a/n	Licensed microwave links, fixed satellite systems, and mobile services	802.11ad/ay
3GPP Releases	Release 16 (5G NR-U)	Release 10/11/12 (LTE-U), Release 13 (LAA), and Release 16 (5G NR-U)	Release 16 (5G NR-U)	Release 16 (5G NR-U)
Available bandwidth	About 100 MHz [47]	500 MHz [7]	500 MHz (Europe) and 1200 MHz (USA) [34]-[35]	9 GHz (Europe) and 14 GHz (the USA)
Spectrum range	2.40-2.50 GHz [47]	5.150-5.925 GHz [7]	5.925-7.125 GHz [5]	57-66 GHz [39]
Antenna pattern	Omnidirectional [34]	Omnidirectional [34]	Omnidirectional [34]	Directional [41]-[42]
Constraints	• Heavily congested • lower data rate	• Lower coverage • Higher penetration and path losses	• Lower coverage • Higher penetration and path losses	• Extremely high penetration and path losses • Blocking
Advantages	• Most utilized unlicensed shared band • Favorable signal propagation characteristics	• Availability of a large amount of spectrum bandwidth • The majority of IEEE 802.11-based technologies operate in this band	• No unlicensed devices now operate [23] • The high capacity demand of future mobile networks can be addressed	• Large spectrum bandwidth availability • High capacity and data rates at a short distance indoors

 ISBN: 978-1-61208-895-2

technology, an MNO can configure its indoor small cells to offload all or a major portion of its user traffic over the unlicensed spectrum, whereas to serve its control signals over the licensed spectrum, when its user traffic demand is high. If, however, indoor small cells of an MNO are not CA enabled, in that case, its small cells can serve only the user data traffic over the unlicensed spectrum, whereas its macrocell can serve the control signals over the licensed spectrum, given that proper coordination exists between the macrocell and indoor small cells of the MNO.

3) Cost-efficiency: Spectrum licensing fee is very expensive and contributes a great portion to the cost to transmit per bit, i.e. cost efficiency, of an MNO. As there is no cost from using an unlicensed spectrum, by operating an MNO in both the licensed and unlicensed spectrum bands, the demand for high capacity and data rates per user of the MNO can be served at a low average cost per bit transmission, resulting in improving its cost-efficiency.

B. Challenges to Operate in the Unlicensed Bands

Several technical challenges remain unaddressed across different layers for the operation of cellular standards (i.e., LTE-U, LAA, and NR-U) and IEEE 802.11 standards (i.e., WiFi and WiGig) in the same unlicensed band. A few noticeable challenges are discussed in the following.

1) Efficient coexistence mechanism: The main challenge to operate cellular standards in the unlicensed band comes from the design of an efficient coexistence mechanism of cellular and IEEE 802.11 standards in the unlicensed band. Major constraints to designing an efficient coexistence mechanism include the lack of inter-Radio Access Technology (RAT) coordination, intercell interference management, independent resource allocations from one RAT to another, and different Medium Access Control (MAC) and Physical Layer (PHY) protocols [31].

2) Physical and MAC layer procedures of cellular and IEEE 802.11 technologies: Though 3GPP based cellular and IEEE 802.11 technologies use the same Orthogonal Frequency Division Multiplexing (OFDM) and Multiple-Input Multiple-Output (MIMO) techniques in the physical layer, other features, including the transmission power, Modulation and Coding Scheme (MCS), and error correction code, are different [48]. Moreover, cellular standards use Radio Link Control Layer with Hybrid Automatic Repeat Request (HARQ), whereas, WiFi, for example, uses Automatic Repeat Request (ARQ) mechanisms, for the recovery of packet losses.

Further, in the case of the MAC layer procedure, cellular technology is an allocation-based mechanism, whereas an IEEE 802.11 (e.g., WiFi) technology is a contention-based mechanism. Cellular technology uses continuous transmission of data in consecutive frames using a centralized scheduler. But, a WiFi technology uses opportunistic transmission using Distributed Coordination Function (DCF). DCF uses the CSMA/CA protocol to detect the energy level in order to get access to a channel. Due to the CSMA/CA behavior, once WiFi APs gain channel access, they occupy the entire bandwidth for a certain amount of time. Conversely, in a cellular technology such as LTE, the bandwidth is first divided into Resource Blocks (RBs), which are then allocated to its users at each Transmission Time Interval (TTI) by a centralized scheduler [49]. Due to these disparities given above in the MAC layer procedures, CCI between a WiFi AP and a cellular node occurs when both accessing the same unlicensed spectrum.

3) Interference management: Since no interference management exists between cellular and IEEE 802.11 standards, and the current LBT does not allow neighboring cellular nodes to transmit simultaneously due to employing contention-based opportunistic scheduling, no simultaneous transmission of cellular and IEEE 802.11 nodes are allowed, and hence no reuse of the same unlicensed spectrum spatially is possible.

4) Transmission mode: Unlike licensed bands, transmissions in unlicensed bands are discontinuous and opportunistic, particularly, for cellular standards using LBT such as LAA and NR-U, which result in reduced efficiency and flexibility in Radio Resource Management (RRM).

5) Beam-based transmissions: Unlike LTE-U and LAA, since NR-U operates as well in the 60 GHz mmWave band using beam-based transmissions, LBT used in LAA with omnidirectional transmissions needs additional requirements to be addressed for the beam-based NR-U.

V. CONCLUSION

This paper has presented an essential survey on unlicensed spectrum bands considered for the operation of cellular mobile networks. Particularly, both sub-7 GHz (i.e., 2.4 GHz, 5 GHz, and 6 GHz) bands and millimeter-wave bands (i.e., 60 GHz) proposed for the Fifth-Generation (5G) and beyond networks have been discussed. Each unlicensed band has been surveyed taking into account the classification, operational region, regulatory requirement, existing technology, available bandwidth, spectrum range, benefit, and challenge. A comparative framework in a tabular form has been developed for numerous aspects to compare one unlicensed band to another to find an appropriate unlicensed spectrum band corresponding to a particular aspect. Finally, we have pointed out major benefits and challenges to operate cellular networks in unlicensed bands.

This paper can serve as a source of fundamental knowledge on unlicensed spectrum bands for cellular technologies and be useful for those who aim at working on the operation of cellular networks in the unlicensed spectrum bands. For more details, interested readers are recommended to refer to the existing works cited throughout the paper and given in the reference section.

REFERENCES

[1] R. K. Saha, “Countrywide Mobile Spectrum Sharing with Small Indoor Cells for Massive Spectral and Energy

Efficiencies in 5G and Beyond Mobile Networks", Energies, vol. 12, no. 20, Art. No. 3825, 2019.

[2] R. K. Saha, "On Maximizing Energy and Spectral Efficiencies using Small Cells in 5G And Beyond Networks," Sensors, vol. 20, no. 6, art. No. 1676, 2020.

[3] Y. Huang, Y. Chen, Y. T. Hou, W. Lou, and J. H. Reed, "Recent Advances of LTE/Wifi Coexistence in Unlicensed Spectrum," IEEE Netw., vol. 32, no. 2, pp. 107-113, March-April 2018.

[4] S. Lagen, N. Patriciello, and L. Giupponi, "Cellular and Wi-Fi in Unlicensed Spectrum: Competition Leading to Convergence," Proc. 2020 2nd 6G Wireless Summit (6G SUMMIT), Levi, Finland, 17-20 Mar. 2020, pp. 1-5.

[5] S. Lagen et al., "New Radio Beam-Based Access to Unlicensed Spectrum: Design Challenges And Solutions," IEEE Commun. Surveys Tuts., vol. 22, no. 1, pp. 8-37, 1st Quart. 2020.

[6] M. Hirzallah, M. Krunz, B. Kecicioglu, and B. Hamzeh, "5G New Radio Unlicensed: Challenges and Evaluation," IEEE Trans. Cogn. Commun. Netw., Dec. 2020.

[7] G. Naik, J. Liu, and, J. J. Park, "Coexistence of Wireless Technologies In The 5 Ghz Bands: A Survey of Existing Solutions and a Roadmap For Future Research," IEEE Commun. Survey Tuts., vol. 20, no. 3, pp. 1777-1798, 3rd Quart. 2018.

[8] R. Zhang et al., "LTE-Unlicensed: The Future of Spectrum Aggregation for Cellular Networks," IEEE Wirel. Commun., vol. 22, no. 3, pp. 150-159, June 2015.

[9] A. Bhorkar, C. Ibars, A. Papathanassiou, and P. Zong, "Medium Access Design for LTE in Unlicensed Band," Proc. 2015 IEEE Wireless Communications and Networking Conference Workshops (WCNCW), New Orleans, LA, USA, 9-12 Mar. 2015, pp. 369-373.

[10] 3GPP, "3rd generation partnership project; evolved universal terrestrial radio access (E-UTRA); further advancements for E-UTRA physical layer aspects (Rel 9)" 3GPP, Sophia Antipoles, France, TR 36.814, V9.0.0, Mar. 2010.

[11] P. Xia, Z. Teng, and J. Wu, "How Loud to Talk and How Hard To Listen-Before-Talk In Unlicensed LTE," Proc. 2015 IEEE International Conference on Communication Workshop (ICCW), London, UK, 8-12 June 2015, pp. 2314-2319.

[12] O. Sallent, J. Pérez-Romero, R. Ferrús, and R. Agustí, "Learning-Based Coexistence For LTE Operation In Unlicensed Bands," Proc. 2015 IEEE International Conference on Communication Workshop (ICCW), 8-12 June 2015, pp. 2307-2313.

[13] Alcatel-Lucent, Ericsson, Qualcomm Technologies Inc., and Samsung Electronics & Verizon, "LTE-U technical report coexistence study for LTE-U SDL V1.3," Technical Report, Nov. 2015. [Online]. Available: http://www.lteuforum.org/uploads/3/5/6/8/3568127/lte-u_forum_lte-u_sdl_coexistence_specifications_v1.3.pdf [retrieved: August 2021]

[14] K. Sadek, T. Kadous, K. Tang, H. Lee, and M. Fan, "Extending LTE to unlicensed band - Merit and coexistence," Proc. 2015 IEEE International Conference on Communication Workshop (ICCW), London, UK, 8-12 June 2015, pp. 2344-2349.

[15] R. K. Saha, "On Operating 5G New Radio Indoor Small Cells In The 60 GHz Unlicensed Band," unpublished, Proc. the Seventeenth International Conference on Wireless and Mobile Communications (ICWMC), Nice, France, 18-22 July 2021.

[16] S. Chatterjee, M. J. Abdel-Rahman, and A. B. MacKenzie, "Optimal Distributed Allocation of Almost Blank Subframes for LTE/WiFi coexistence," Proc. 2017 15th International Symposium on Modeling and Optimization in Mobile, Ad Hoc, and Wireless Networks (WiOpt), Paris, France, 15-19 May 2017, pp. 1-6.

[17] R. K. Saha, "Power-Domain Based Dynamic Millimeter-Wave Spectrum Access Techniques For In-Building Small Cells In Multioperator Cognitive Radio Networks Toward 6G," Wirel. Commun. Mob. Comput., vol. 2021, Art. ID 6628751, 2021.

[18] F. M. Abinader et al., "Enabling The Coexistence Of LTE And Wi-Fi In Unlicensed Bands," IEEE Commun. Mag., vol. 52, no. 11, pp. 54-61, Nov. 2014.

[19] F. S. Chaves et al., "LTE UL power control for the improvement of LTE/Wi-Fi coexistence," Proc. 2013 IEEE 78th Vehicular Technology Conference (VTC Fall), Las Vegas, NV, USA, 2-5 Sep. 2013, pp. 1-6.

[20] B. Chen, J. Chen, Y. Gao, and J. Zhang, "Coexistence of LTE-LAA and Wi-Fi on 5 GHz with corresponding deployment scenarios: a survey," IEEE Commun. Surveys Tuts., vol. 19, no. 1, pp. 7-32, 1st Quart. 2017.

[21] V. Sathya, M. I. Rochman, and M. Ghosh, "Hidden-Nodes in Coexisting LAA & Wi-Fi: A Measurement Study of Real Deployments," Proc. 2021 IEEE International Conference on Communications Workshops (ICC Workshops), Montreal, QC, Canada, 2021, pp. 1-7.

[22] S. M. Kala, V. Sathya, E. Yamatsuta, H. Yamaguchi, T. Higazhino, "Operator Data Driven Cell-Selection in LTE-LAA Coexistence Networks" Proc. ICDCN '21: International Conference on Distributed Computing and Networking, Nara, Japan, January 2021, pp. 206-214.

[23] G. Naik, J. -M. Park, J. Ashdown, and W. Lehr, "Next Generation Wi-Fi And 5G NR-U In The 6 Ghz Bands: opportunities and challenges," IEEE Access, vol. 8, pp. 153027-153056, 2020.

[24] C. J. Hansen, "WiGiG: Multi-gigabit Wireless Communications in The 60 GHz Band," IEEE Wirel. Commun., vol. 18, no. 6, pp. 6-7, Dec. 2011.

[25] V. Sathya, M. I. Rochman, and M. Ghosh, "Measurement-Based Coexistence Studies of LAA & Wi-Fi Deployments in Chicago," IEEE Wireless Communications, vol. 28, no. 1, pp. 136-143, February 2021.

[26] M. I. Rochman et al., "A Comparison Study of Cellular Deployments in Chicago and Miami Using Apps on Smartphones Available online: https://arxiv.org/abs/2108.00453 [retrieved: August 2021]

[27] A. Al-Dulaimi, S. Al-Rubaye, Q. Ni, and E. Sousa, "5G Communications Race: Pursuit of More Capacity Triggers LTE in Unlicensed Band," IEEE Veh. Technol. Mag., vol. 10, no. 1, pp. 43-51, 2015.

[28] R. Ratasuk, N. Mangalvedhe, and A. Ghosh, "LTE In Unlicensed Spectrum Using Licensed-Assisted Access," in Proc. 2014 IEEE Globecom Workshops (GC Wkshps), Austin, TX, USA, 8-12 Dec. 2014, pp. 746-751.

[29] R. Kwan et al., "Fair Co-Existence of Licensed Assisted Access LTE (LAA-LTE) and Wi-Fi in unlicensed spectrum," Proc. 2015 7th Computer Science and Electronic Engineering Conference (CEEC), Colchester, UK, 24-25 Sept. 2015, pp. 13-18.

[30] 3GPP, "3rd Generation Partnership Project; TSG RAN; *Study On Licensed-Assisted Access To Unlicensed Spectrum*,"

3GPP, Sophia Antipoles, France, TR 38.889, Release 13, V13.0.0, June 2015.

[31] M. Ali, S. Qaisar, M. Naeem, W. Ejaz, and N. Kvedaraite, "LTE-U WiFi Hetnets: Enabling Spectrum Sharing For 5G/Beyond 5G Systems," IEEE Internet Things Mag., vol. 3, no. 4, pp. 60-65, Dec. 2020.

[32] List of WLAN channels. [Online]. Available: https://en.wikipedia.org/wiki/List_of_WLAN_channels. [retrieved: August, 2021].

[33] *Mandate to CEPT to Study Feasibility and Identify Harmonized Technical Conditions for Wireless Access Systems Including Radio Local Area Networks in the 5925–6425 MHz Band for the Provision of Wireless Broadband Services*, Dec. 2017, [online] Available: http://ec.europa.eu/newsroom/dae/document.cfm?doc_id=50343. [retrieved: August, 2021].

[34] Federal Communications Commission, "Fact Sheet: Unlicensed Use of the 6 GHz Band Notice of Proposed Rulemaking," no. 18-295, Oct. 2018. [Online]. Available: https://docs.fcc.gov/public/attachments/DOC-354364A1.pdf [retrieved: August 2021]

[35] *Notice of proposed rulemaking; in the matter of unlicensed use of the 6 GHz band (ET Docket No. 18–295); expanding flexible use in mid-band spectrum between 3.7 and 24 GHz (GN Docket No. 17–183)*, Oct. 2018. [online]. Available: https://docs.fcc.gov/public/attachments/FCC-18-147A1.pdf.

[36] Z. Pi and F. Khan, "An Introduction To Millimeter-Wave Mobile Broadband Systems," IEEE Commun. Mag., vol. 49, no. 6, pp. 101-107, June 2011.

[37] J. G. Andrews, T. Bai, M. N. Kulkarni, A. Alkhateeb, A. K. Gupta, and R. W. Heath, "Modeling and analyzing millimeter wave cellular systems", *IEEE Trans. Commun.*, vol. 65, no. 1, pp. 403-430, Jan. 2017.

[38] IEEE_802.11ad. [Online]. Available: https://en.wikipedia.org/wiki/IEEE_802.11ad [retrieved: August 2021]

[39] C. J. Hansen, "WiGiG: Multi-gigabit Wireless Communications in the 60 GHz band," IEEE WIREL. COMMUN., vol. 18, no. 6, pp. 6-7, Dec. 2011.

[40] C. Rosa, M. Kuusela, F. Frederiksen, and K. I. Pedersen, "Standalone LTE in Unlicensed Spectrum: Radio Challenges, Solutions, And Performance Of Multefire," IEEE Commun. Mag., vol. 56, no. 10, pp. 170-177, Oct. 2018.

[41] Federal Communications Commission, "Fact sheet: Spectrum frontiers rules identify, open up vast amounts of new high-band spectrum for next generation (5G) wireless broadband," no. 340310A1, June 2016. [Online]. Available: https://www.fcc.gov/document/fact-sheet-spectrum-frontiers-item [retrieved: August 2021]

[42] "5G Spectrum Recommendations." White Paper, 5G Americas, Bellevue, WA, USA, Apr. 2017. [Online]. Available: https://www.5gamericas.org/wp-content/uploads/2019/07/5GA_5G_Spectrum_Recommendations_2017_FINAL.pdf [retrieved: August 2021]

[43] *Regulatory guidelines for use of 2.4 GHz ism band for commercial services in lesotho*, Lesotho Communications Authority, June 2014. [Online]. [Available]: https://www.lca.org.ls/wp-content/uploads/2019/03/ISM-BAND-GUIDELINES-11022015.pdf [retrieved: August 2021]

[44] H. Kwon et al., "Licensed-assisted access to unlicensed spectrum in LTE Release 13," IEEE Commun. Mag., vol. 55, no. 2, pp. 201-207, Feb. 2017.

[45] *60 GHz Band Regulation*. [Online]. Available: https://www.60ghz-wireless.com/60ghz-technology/60ghz-band-regulation/ [retrieved: August 2021]

[46] *60 GHz-tech-overview*. [Online]. Available: https://www.lightpointe.com/60ghz-tech-overview [retrieved: August 2021]

[47] 2.4 GHz radio use. [Online]. Available: https://en.wikipedia.org/wiki/2.4_ghz_radio_use [retrieved: August 2021]

[48] E. Baena, S. Fortes, and R. Barco, "KQI Performance Evaluation of 3GPP LBT Priorities for Indoor Unlicensed Coexistence Scenarios," Electronics, vol. 9, Art. No. 1701, 2020.

[49] T. Nihtilä et al., "System Performance of LTE and IEEE 802.11 Coexisting On A Shared Frequency Band," Proc. 2013 IEEE Wireless Communications And Networking Conference (WCNC), Shanghai, China, 7-10 Apr. 2013, pp. 1038-1043.

 ISBN: 978-1-61208-895-2

On Operating Cellular Technologies in Unlicensed Spectrum Bands: A Review

Rony Kumer Saha
Radio and Spectrum Laboratory
KDDI Research, Inc.
2-1-15 Ohara, Fujimino-shi, Saitama 356-8502, Japan
email: ro-saha@kddi-research.jp

***Abstract*—In this paper, we provide a brief, yet reasonably broad in scope, review on the coexistence of cellular and IEEE 802.11 standards, which takes into account the coexistence of all existing and future cellular standards in all available unlicensed spectrum bands. In particular, the paper summarizes key things, including coexistence fairness, related features, regulatory requirements, design principles, mechanisms, deployment scenarios, challenges, and convergence, necessary for the coexistence of cellular technologies in the unlicensed bands.**

Keywords-Unlicensed band; review; cellular network; WiFi; coexistence.

I. INTRODUCTION

The scarcity of radio spectrum has been a major bottleneck in cellular mobile communications [1]. An increase in high capacity and data rate demands due to the recent growth of mobile data traffic puts a further burden on the licensed spectrum of a Mobile Network Operator (MNO). Even though several attempts have been taken to address the spectrum scarcity issue, e.g., improving the utilization of the licensed spectrum, the situation has not been improved considerably. This causes MNOs to seek alternative solutions, and operating as well in the unlicensed bands has been found effective due to the availability of a large amount of spectrum in the unlicensed bands.

Numerous studies [2]-[6] have already been carried on the coexistence of cellular and Institute of Electrical and Electronics Engineers (IEEE) 802.11 standards taking into account one or more of the following aspects, including the unlicensed spectrum band, coexistence mechanism, transmission mode, deployment scenario, regulatory requirement, design principle, and potential issue. For example, the authors in [3] studied Long-Term Evolution (LTE)-Licensed Assisted Access (LAA) and Wireless Fidelity (WiFi) coexistence in the 5 GHz with the corresponding deployment scenario. Similarly, in [4], the authors presented a coexistence study of Wi-Fi and LTE-in-unlicensed by surveying a large parameter space of coexistence mechanisms and a range of representative network densities and deployment scenarios. Nevertheless, in [5], emphasizing unlicensed Millimeter-Wave (mmWave) bands, as well as considering the beam-based transmissions, the authors presented an overview of the major design principles and solutions to operate New Radio Unlicensed (NR-U) in unlicensed bands.

Different from these above studies, in this paper, we provide a brief review on the coexistence of cellular and IEEE 802.11 standards by taking into account the coexistence of all existing and future cellular standards in all available unlicensed bands. Based on the existing literature, fundamental aspects for the coexistence of these two established wireless technologies**,** including coexistence fairness, related features, regulatory requirements, design principles, mechanisms, deployment scenarios, challenges, and convergence, are summarized. The detailed discussion on each aspect of the above aspects is out of the scope of this paper. However, for further information, a list of references is given in the end so that interested readers may refer to these references corresponding to any fundamental aspect mentioned alongside while discussing in this paper.

The paper is organized as follows. Section II covers the discussion on the available unlicensed bands for the operation of cellular technologies. The condition for fair coexistence, as well as coexistence-related features, are discussed in Section III. Coexistence mechanisms and deployment scenarios are reviewed in Section IV and Section V, respectively. Finally, we highlight technical challenges and convergence of coexistence in Section VI. We conclude the review in Section VII.

II. CELLULAR TECHNOLOGIES IN UNLICENSED BANDS

Cellular technologies may operate in one or more unlicensed spectrum bands, including 2.4 GHz, 5 GHz, 6 GHz, and 60 GHz. Due to the similar propagation characteristics, 2.4 GHz, 5 GHz, and 6 GHz are termed as sub-7 GHz, whereas 60 GHz as mmWave, bands. The first cellular-based technology extended with a view to operating only in the 5 GHz unlicensed spectrum is the Fourth-Generation (4G) LTE in 2015. The two variants of LTE in the unlicensed band are LTE Unlicensed (LTE-U) in the Third Generation Partnership Project (3GPP) Release 12 [7] and LAA in 3GPP Releases 13, 14, and 15 [8]-[12].

However, operations in the mmWave have been permitted recently starting first with the Fifth-Generation (5G) NR-U [5], [13] technology in 3GPP Release 16.

 ISBN: 978-1-61208-895-2

Recently, Federal Communications Commission (FCC) approved the 6 GHz band in the USA for spectrum sharing [14]. Likewise, Europe is considering allowing the 6 GHz band to use [15]. In line with so, 3GPP has recently released the specifications for NR-U in Release 16 where the provision for NR-U devices to operate in the 6 GHz band is incorporated [5], [16]. Hence, unlike LTE-U and LAA, NR-U supports multiple unlicensed bands, including sub-7 GHz and mmWave bands.

III. COEXISTENCE FAIRNESS AND RELATED FEATURE

A major concern that is faced by each cellular technology is the Co-Channel Interference (CCI) from the incumbent IEEE 802.11 technologies operating in these unlicensed bands. This requires a proper and fair coexistence of cellular with IEEE 802.11 technologies. Though there is no concrete definition for fair coexistence, according to the 3GPP, the fair coexistence between a cellular network such as LTE and an IEEE 802.11 network such as WiFi is defined as follows: *The capability of an LAA network not to impact WiFi networks active on a carrier more than an additional WiFi network operating on the same carrier, in terms of throughput and latency* [17], [18]. Likewise, for NR-U, the coexistence requirement with WiFi/Wireless Gigabit (WiGig) remains the same as that in LAA [16]. However, it is to be noted that many 3GPP members might believe that fairness means cellular nodes and IEEE 802.11 Access Points (APs) should have half of the bandwidth.

Developing a coexistence mechanism is challenging and hence knowledge about the coexistence-related features of both technologies, namely channel access mechanisms, Medium Access Control (MAC) protocols, design principles, and regulatory requirements, reasoned as follows, are crucial.

- *Channel access mechanisms*: Since cellular technologies do not listen to the channel condition when scheduling resources and IEEE 802.11 technologies use the contention-based protocol to access a channel, it is not unusual that cellular nodes may block transmission of WiFi APs completely [3].
- *MAC protocols*: Cellular technology uses continuous transmission of data in consecutive frames using a centralized scheduler. However, WiFi technology uses opportunistic transmission using the Carrier-Sense Multiple Access with Collision Avoidance (CSMA/CA) protocol [7] to get access to an unlicensed channel. Due to this disparity in MAC layer procedures, WiFi APs may get blocked by a cellular node as the interference level of a cellular network is likely to be above the threshold used by a WiFi network to detect the vacancy of a channel. Likewise, Because WiFi packets are transmitted always with maximum power, if WiFi APs can get access to a channel, they can cause interference to a cellular network.
- *Design principles*: Cellular technology, such as LTE is designed with an assumption that LTE can transmit with a small-time gap continuously and periodically. However, WiFi is designed to coexist with other technologies through random backoff and channel sensing, which allows a WiFi AP a little chance to sense a clear channel and transmit. Due to this reason, a WiFi AP moves to the silence mode causing its performance degradations, while any LTE node remains almost unaffected [3].
- *Regulatory requirements*: Regulatory requirements to operate different cellular technologies in unlicensed bands vary from one country or region to another. For example, though countries such as the USA, China, India, and South Korea [3] do not require cellular technologies such as LTE to be Listen-Before-Talk (LBT) enabled, LBT is mandatory in Japan and Europe. LBT is a contention-based medium access technique similar to the CSMA/CA mechanism used by WiFi [5], meaning that LBT does not allow a cellular node to occupy a channel at all times. Since LTE-U does not implement the LBT mechanism, it can be used in the USA, China, India, and South Korea. Instead, as LAA is LBT enabled, LAA can be used worldwide [3].

IV. COEXISTENCE MECHANISM

Coexistence mechanisms can be developed in two ways depending on whether or not modifications on the existing cellular networks are employed. If modifications are employed, a cellular network is enabled with the LBT mechanism to avoid CCI with other existing transmissions by backing off or moving to another channel. LBT shares a channel between a cellular node and a WiFi AP fairly [7] by enabling a cellular node to stop periodically its channel occupancy and to detect the activities of other shared nodes at a millisecond-level [7] to avoid CCI. Since LAA is LBT enabled, this approach is used in LAA.

On the other hand, if modifications are not employed, a cellular network cannot be enabled with LBT. Numerous coexistence mechanisms without employing LBT have been proposed by exploiting different domains to manage CCI, particularly, Channel Selection (CHS) in frequency-domain [19], [20], Carrier Sense Adaptive Transmission (CSAT) [20], [21] and Fully Blank Subframe (FBS) [22], [23] in time-domain, and Transmit Power Control (TPC) in power-domain [24], [25], [26]. A key feature of each of these mechanisms is that none requires modifications on existing cellular networks.

In the frequency and time domains, the principle of coexistence is based on maintaining the orthogonal transmission of each coexisting node in frequency and time, respectively [27], [28], [29]. In other words, only one node, i.e., either a WiFi AP or a cellular node, can transmit at a time to avoid a collision. However, in the power domain, CCI can be controlled by applying the power control

 ISBN: 978-1-61208-895-2

method (i.e., adjusting the output power) to cellular nodes [24], [25], [26]. As LTE-U is not LBT enabled, this approach can be used in LTE-U by exploiting any domain.

Besides, since in practice, the WiFi traffic is bursty, it results in a huge amount of white spaces between WiFi frames. WiFi white spaces create a huge source of spectrum for cellular technologies such as LTE-U [30] that can exploit these white spaces to transmit opportunistically. In this regard, Markov Modulated Batch Poisson Process Model [30] and Reinforcement Learning Technique [31] are examples of approaches to exploit WiFi white spaces. Further, Neural Networks Technology [32] and Graph-based mechanisms [33] can also be employed to enable the coexistence between cellular and IEEE 802.11 technologies in the unlicensed spectrum.

V. COEXISTENCE DEPLOYMENT SCENARIO

Because the supported enabling technologies, including Carrier Aggregation (CA), Dual Connectivity (DC), and standalone operation, of one cellular standard vary from the other, coexistence deployment scenarios of cellular standards vary accordingly. For example, using the CA technology, three deployment scenarios for LTE-U standard in heterogeneous networks [34] and four deployment scenarios for Small Cells (SCs) in LAA [35] are defined by 3GPP. Since NR-U can exploit the DC and standalone operation additionally, five deployment scenarios are defined by 3GPP for NR-U [16], [36].

It is to be noted that DC and CA modes play major roles in connecting User Equipments (UEs) over unlicensed bands. In DC, data of a UE can be exchanged simultaneously with more than one Next Generation NodeBs (gNBs)/Evolve NodeBs (eNBs) [36]. However, in the CA, data of a UE can be exchanged simultaneously with a gNB/eNB through multiple contiguous or noncontiguous bands [36]. Due to this reason, while the CA can help improve the throughput, the DC can improve throughput, as well as reliability. Moreover, in the DC, failure of the primary link does not impact the secondary links [36]. This implies a major improvement for the deployment of NR in unlicensed bands with respect to that of LTE-U and LAA. In Table I, numerous aspects of 3GPP-based different cellular standards are compared.

VI. COEXISTENCE CHALLENGE AND CONVERGENCE

A. Coexistence Challenge

Several technical challenges remain unaddressed across different layers for the coexistence of cellular standards and IEEE 802.11 standards. Few key challenges are as follows.

- The main challenge for the coexistence of cellular and IEEE 802.11 standards comes from the major constraints to design an efficient coexistence mechanism, including the lack of inter-Radio Access Technology (RAT) coordination, intercell interference management, independent resource allocations from one RAT to another, and different MAC and Physical Layer (PHY) protocols [34].

TABLE I
COMPARISON OF NUMEROUS ASPECTS OF DIFFERENT CELLULAR STANDARDS

Aspect	LTE-U	LAA	NR-U
Standardized Bodies	3GPP and LTE-U Forum	3GPP	
Deployment mode	CA		CA, DC, and Standalone
Unlicensed bands	5 GHz		2.4 GHz, 5 GHz, 6 GHz, and 60 GHz
Coexistence mechanism	CHS, FBS, CSAT, and TPC	LBT	
Usage regions	The USA, China, South Korea	Worldwide	
3GPP Release	12	13, 14, and 15	18

- There exists a continuous dispute over the effectiveness of the existing coexistence mechanisms. For example, CSAT/FBS suffer from their weaknesses, i.e., ON/OFF periods for the duty-cycle of CSAT and non-blank subframe duration of an FBS pattern period are controlled by the cellular node, and WiFi APs adapt to this change, resulting in poor WiFi performances [3].
- In unlicensed bands, no interference management like in the licensed bands exists between cellular and IEEE 802.11 standards. Moreover, the current LBT does not allow neighboring cellular nodes to transmit simultaneously due to employing the contention-based opportunistic scheduling [37]. These result in allowing no simultaneous transmission of cellular and IEEE 802.11 nodes, and hence no reuse of the same unlicensed spectrum spatially.
- Unlike licensed bands, transmissions in unlicensed bands are discontinuous and opportunistic, particularly, for cellular standards using LBT such as LAA and NR-U, which result in reduced efficiency and flexibility in Radio Resource Management (RRM) [37].
- Interference scenarios in unlicensed bands are not predictable [37], resulting in increasing received interference signals due to opportunistic channel access from WiFi.
- Unlike LTE-U and LAA, since NR-U operates as well in the 60 GHz mmWave band, using beam-based transmissions [5], LBT used in LAA with omnidirectional transmissions needs additional requirements to be addressed for beam-based NR-U.

B. Coexistence Convergence

Even though they differ in numerous critical features and compete with each other to access unlicensed bands, from the latest versions of the IEEE 802.11ax and 3GPP NR-U, it can be found that both technologies are converging

 ISBN: 978-1-61208-895-2

to use large bandwidth in terms of aspects used in the radio access by introducing the best of both standards [13]. For example, WiFi has introduced cellular features such as Hybrid Automatic Repeat Request (HARQ) and Orthogonal Frequency-Division Multiplexing (OFDM). Likewise, NR-U adopts a short-length frame structure, flexible access, and LBT protocol used in WiFi to get adapt to the characteristics of unlicensed bands [13].

VII. CONCLUSION

In this paper, we have given a brief review of fundamental aspects for the coexistence of cellular and IEEE 802.11 standards. Unlike existing studies, the coexistence of all existing and future cellular standards in all available unlicensed spectrum bands has been considered. We have covered reasonably broad features necessary to understand the coexistence of cellular technologies in the unlicensed bands, including coexistence fairness, related features, regulatory requirements, design principles, mechanisms, deployment scenarios, challenges, and convergence, concisely. Based on the existing literature, the review in this paper aims at introducing readers to the key aspects for the coexistence of these two established wireless technologies in unlicensed bands.

REFERENCES

[1] R. K. Saha, "On Maximizing Energy and Spectral Efficiencies Using Small Cells in 5G and Beyond Networks," Sensors, vol. 20, no. 6, art no. 1676, 2020.

[2] J. Zhang et al., "LTE on License-Exempt Spectrum," IEEE Commun. Surveys Tuts., vol. 20, no. 1, pp. 647-673, 1st Quart. 2018.

[3] B. Chen, J. Chen, Y. Gao, and J. Zhang, "Coexistence of LTE-LAA and Wi-Fi on 5 GHz with Corresponding Deployment Scenarios: A Survey," IEEE Commun. Surveys Tuts., vol. 19, no. 1, pp. 7-32, 1st Quart. 2017.

[4] L. Simić, A. M. Voicu, P. Mähönen, M. Petrova, and J. P. De Vries, "LTE in Unlicensed Bands Is Neither Friend Nor Foe to Wi-Fi," IEEE Access, vol. 4, pp. 6416-6426, 2016.

[5] S. Lagen et al., "New Radio Beam-Based Access to Unlicensed Spectrum: Design Challenges And Solutions," IEEE Commun. Surveys Tuts., vol. 22, no. 1, pp. 8-37, 1st Quart. 2020.

[6] G. Naik, J. -M. Park, J. Ashdown, and W. Lehr, "Next Generation Wi-Fi And 5G NR-U In The 6 Ghz Bands: Opportunities And Challenges," IEEE Access, vol. 8, pp. 153027-153056, 2020.

[7] R. Zhang et al., "LTE-Unlicensed: The Future of Spectrum Aggregation For Cellular Networks," IEEE Wirel. Commun., vol. 22, no. 3, pp. 150-159, June 2015.

[8] 3GPP, "3rd Generation Partnership Project; TSG RAN; Study On Licensed Assisted Access To Unlicensed Spectrum," 3GPP, Sophia Antipoles, France, TR 36.889, Release 13, V13.0.0, June 2015.

[9] H. Kwon et al., "Licensed-Assisted Access To Unlicensed Spectrum In LTE Release 13," IEEE Commun. Mag., vol. 55, no. 2, pp. 201-207, Feb. 2017.

[10] A.-K. Ajami and H. Artail, "On The Modeling And Analysis Of Uplink And Downlink IEEE 802.11ax Wi-Fi With LTE In Unlicensed Spectrum", IEEE Trans. Wireless Commun., vol. 16, no. 9, pp. 5779-5795, Sep. 2017.

[11] M. Mehrnoush, V. Sathya, S. Roy, and M. Ghosh, "Analytical modeling of Wi-Fi and LTE-LAA coexistence: Throughput and impact of energy detection threshold", IEEE/ACM Trans. Netw., vol. 26, no. 4, pp. 1990-2003, Aug. 2018.

[12] A. D. Shoaei, M. Derakhshani, and T. Le-Ngoc, "Efficient LTE/Wi-Fi Coexistence In Unlicensed Spectrum Using Virtual Network Entity: Optimization And Performance Analysis," IEEE Trans. Commun., vol. 66, no. 6, pp. 2617-2629, Jun. 2018.

[13] S. Lagen, N. Patriciello, and L. Giupponi, "Cellular and Wi-Fi in Unlicensed Spectrum: Competition Leading To Convergence," Proc. 2020 2nd 6G Wireless Summit (6G SUMMIT), Levi, Finland, 17-20 Mar. 2020, pp. 1-5.

[14] G. Naik, and J. M. Park, "Coexistence of Wi-Fi 6E and 5G nr-u: Can we do better in the 6 GHz bands?" [online] available: https://winser.ece.vt.edu/wp-content/uploads/2020/12/Infocom_2021_WiFi6__5G-NR-U.pdf [retrieved: August 21, 2021]

[15] *Mandate to CEPT to Study Feasibility and Identify Harmonized Technical Conditions for Wireless Access Systems Including Radio Local Area Networks in the 5925–6425 MHz Band for the Provision of Wireless Broadband Services*, Dec. 2017, [online] Available: http://ec.europa.eu/newsroom/dae/document.cfm?doc_id=50343. [retrieved: August 21, 2021]

[16] 3GPP, "3rd generation partnership project; TSG RAN; study on NR-based access to unlicensed spectrum," 3GPP, Sophia Antipoles, France, TR 38.889, Release 16, V16.0.0, Dec. 2018.

[17] R. Ratasuk, N. Mangalvedhe, and A. Ghosh, "LTE In Unlicensed Spectrum Using Licensed-Assisted Access," Proc. 2014 IEEE Globecom Workshops (GC Wkshps), Austin, TX, USA, 8-12 Dec. 2014, pp. 746-751.

[18] R. Kwan et al., "Fair Co-Existence Of Licensed Assisted Access LTE (LAA-LTE) and Wi-Fi In Unlicensed Spectrum," Proc. 2015 7th Computer Science and Electronic Engineering Conference (CEEC), Colchester, UK, 24-25 Sept. 2015, pp. 13-18.

[19] O. Sallent, J. Pérez-Romero, R. Ferrús, and R. Agustí, "Learning-Based Coexistence For LTE Operation In Unlicensed Bands," Proc. 2015 IEEE International Conference on Communication Workshop (ICCW), 8-12 June 2015, pp. 2307-2313.

[20] S. K. Ahmed, "Carrier Sense Adaptive Transmission (CSAT) in Unlicensed Spectrum," US Patent No. US 9,491,632 B2, Nov. 8, 2016.

[21] A. K. Sadek, T. Kadous, K. Tang, H. Lee, and M. Fan, "Extending LTE to Unlicensed Band - Merit and Coexistence," Proc. 2015 IEEE International Conference on Communication Workshop (ICCW), London, UK, 8-12 June 2015, pp. 2344-2349.

[22] R. K. Saha, "On Operating 5G New Radio Indoor Small Cells In The 60 Ghz Unlicensed Band," unpublished, *Proc.* the Seventeenth International Conference on Wireless and Mobile Communications (ICWMC), Nice, France, 18-22 July 2021.

[23] S. Chatterjee, M. J. Abdel-Rahman, and A. B. MacKenzie, "Optimal Distributed Allocation Of Almost Blank Subframes For LTE/Wifi Coexistence," Proc. 2017 15th International Symposium On Modeling and Optimization in Mobile, Ad

 ISBN: 978-1-61208-895-2

Hoc, and Wireless Networks (WiOpt), Paris, France, 15-19 May 2017, pp. 1-6.
[24] R. K. Saha, "A Hybrid Interweave-Underlay Countrywide Millimeter-Wave Spectrum Access And Reuse Technique For CR Indoor Small Cells In 5G/6G Era," Sensors, vol. 20, no. 14, art. no. 3979, 2020.
[25] R. K. Saha, "Millimeter-wave Spectrum Utilization Improvement In Multi-Operator Networks: A Framework Using The Equal Likelihood Criterion," IEEE Access, vol. 9, pp. 72980-72999, 2021.
[26] R. K. Saha, "Power-Domain Based Dynamic Millimeter-Wave Spectrum Access Techniques For In-Building Small Cells In Multioperator Cognitive Radio Networks Toward 6G," Wirel. Commun. Mob. Comput., vol. 2021, art. ID 6628751, 13 pages, 2021.
[27] R. K. Saha, "An Overview And Mechanism For The Coexistence Of 5G Nr-U (New Radio Unlicensed) In The Millimeter-wave spectrum for indoor small cells," unpublished, Wirel. Commun. Mob. Comput., 2021.
[28] R. K. Saha "Spectrum Allocation And Reuse In 5G New Radio On Licensed And Unlicensed Millimeter-Wave Bands In Indoor Environments," Mob. Info. Syst. vol. 2021, art. ID 5538820, pages 21, 2021.
[29] R. K. Saha, "Licensed Countrywide Full-Spectrum Allocation: A New Paradigm For Millimeter-Wave Mobile Systems In 5g/6g era," IEEE Access, vol. 8, pp. 166612-166629, 2020.
[30] N. Rastegardoost and B. Jabbari, "Statistical characterization of wifi white space," IEEE Commun. Lett., vol. 21, no. 12, pp. 2674-2677, Dec. 2017.
[31] N. Rastegardoost and B. Jabbari, "A Machine Learning Algorithm For Unlicensed LTE And Wifi Spectrum Sharing," Proc. 2018 IEEE International Symposium on Dynamic Spectrum Access Networks (DySPAN), Seoul, South Korea, 22-25 Oct. 2018, pp. 1-6.
[32] M. Alsenwi et al., "Towards Coexistence Of Cellular And Wifi Networks In Unlicensed Spectrum: A Neural Networks based approach," IEEE Access, vol. 7, pp. 110023-110034, 2019.
[33] Z. Han, N. Dusit, W. Saad, T. Basar, and A. Hjørungnes, Game theory in Wireless And Communication Networks: Theory, Models, And Applications. Cambridge University Press, 2012.
[34] M. Ali, S. Qaisar, M. Naeem, W. Ejaz, and N. Kvedaraite, "LTE-U WiFi Hetnets: Enabling Spectrum Sharing For 5G/Beyond 5G Systems," IEEE Internet Things Mag., vol. 3, no. 4, pp. 60-65, Dec. 2020.
[35] 3GPP, "3rd generation partnership project; TSG RAN; *study on licensed-assisted access to unlicensed spectrum*," 3GPP, Sophia Antipoles, France, TR 38.889, Release 13, V13.0.0, June 2015.
[36] M. Hirzallah, M. Krunz, B. Kecicioglu, and B. Hamzeh, "5G New Radio Unlicensed: Challenges And Evaluation," IEEE Trans. Cogn. Commun. Netw., Early Access, pp. 1-1, Dec. 2020.
[37] Y. Huang, Y. Chen, Y. T. Hou, W. Lou, and J. H. Reed, "Recent Advances Of LTE/WiFi Coexistence In Unlicensed Spectrum," IEEE Netw., vol. 32, no. 2, pp. 107-113, March-April 2018.

 ISBN: 978-1-61208-895-2

Net-Preflight Check:Using File Transfers to Measure Network Performance before Large Data Transfers

Bashir Mohammed
Scientific Data Management(SDM)
Lawrence Berkeley National Lab
Berkeley,CA, USA
email:bmohammed@lbl.gov

Mariam Kiran
Energy Sciences Network(ESnet)
Lawrence Berkeley National Lab
Berkeley,CA, USA
email:mkiran@es.net

Bjoern Enders
Natl. Energy Research Sci.Comp.Center(NERSC)
Lawrence Berkeley National Lab
Berkeley, CA, USA
email:benders@lbl.gov

***Abstract*—During bulk data transfer for exascale scientific applications, measuring the available throughput is very useful for route selection in high-speed networks, Quality of service verification, and traffic engineering. Recent years have seen a surge in available throughput estimation tools, especially in Research and Education (R&E) Networks. Some tools have been proposed and evaluated in simulation and over a limited number of Internet paths. However, there is still significant uncertainty in the performance and flexibility of these tools at large. Furthermore, some existing tools' primary concern is the lack of network performance history or a memory that stores previous configurations and network measurements. This paper introduces Net-PreFlight, a simple end-to-end, lightweight tool for measuring available throughput, traceroute, and maintains memory, compared to existing tools like Iperf. Our tool focuses on throughput measurements, flexibility, a retentive memory, security, and performance. We conduct experiments between multiple Data Transfer Node (DTN) setups in isolated and public network setups to measure how throughput measurements fare in the two domains. In all scenarios, Net-Preflight produces comparable results as established tools and hence positions itself as a complementary tool for situations where the deployment of Iperf or perfSONAR is not possible. In addition, Net-Preflight features retentive memory to easily compare past and present measurements. Our analysis reveals that using socket and file transfer protocols performs well in initial measurements and also indicates that parallel TCP streams are equivalent to using a large maximum segment size on a single connection in the absence of congestion. Here, we lay the foundation to build a new monitoring system for DTN bulk transfers that target end-users who require optimum network performance.**

***Keywords*—Throughput measurement, Data Transfer, TCP, Network performance monitoring**

I. Introduction

Recent years have seen a strong interest in techniques for estimating available throughput and bandwidth along an Internet network path. The path diversity in R&E or overlay networks creates a need for estimating the available throughput over these paths as a method for choosing the best time and network route before initiating a bulk data transfer [1]. However, in an overlay or traditional network, one can assume the cooperation of both the sender and the receiver, which is necessary for most probing techniques. Available throughput measurement during bulk data transfer for exascale scientific applications is very useful for route selection in overlay networks, Quality of service verification and traffic engineering [2]. A few tools have been proposed and evaluated in simulation and over a limited number of internet paths, but there is still great uncertainty in the performance of these tools over isolated and public network, as well as R&E Networks at large. For instance, Iperf is a popular network monitoring tool for active measurements of the maximum achievable bandwidth on IP networks, and it supports tuning of various parameters related to timing, buffers and protocols, such as TCP and UDP. For each test, Iperf3 reports the bandwidth, loss, and other parameters. However, a major limitation with iperf3 is lack of flexibility because you have to install it at both ends of the measurement (Server-Client), and also lack of retentive memory and performance history which stores previous configurations and network measurements.

Another popular existing tool is the performance Service-Oriented Network monitoring Architecture (perfSONAR) [3], which is a network measurement toolkit designed to provide federated coverage of paths and help to establish end-to-end usage expectations. There are thousands of perfSONAR instances deployed worldwide and many of which are available for open testing of key measures of network performance. It is an essential tool that ensures scientists can rely on networks to get their data from end-to-end as quickly as possible. However, even though perfSONAR provides a uniform interface that allows for the scheduling of measurements, storage of data in uniform formats, as well as scalable methods to retrieve data and generate visualization, it has a similar limitation with Iperf3 because you need to install a perfSONAR instance or node, at both server and client-end, before you can run tests for accurate measurements. It also does not have retentive memory capability, which means users or network engineers are unable to see previous configurations and network performances to compare with current measurements [3].

To bridge this gap, this paper introduces Net-Preflight, a tool intended to indicate the state of the network between two nodes in an overlay, prior to performing large scale data transfers. We summarize our contributions as follows:

- We develop and present Net-Preflight, a custom, simple end-to-end, light-weight tool for measuring available throughput on a well provisioned network.
- We compare and verify Net-Preflight with Iperf focusing on throughput measurement accuracy, security, retentive

 ISBN: 978-1-61208-895-2

memory and performance issues, using different file transfers and utilizing isolated networks as well as the public internet network path for DTN-to-DTN testing.

Please note: the Net-Preflight tool is designed to help end-users sending bulk transfers and need a quick network health check to ensure quality of service. It is not designed to replace Iperf or Perfsonar tools, but rather network checks especially when root access at receiver end is not available.

In the last decade, the US Department of Energy experimental and observational user facilities have seen a huge increase in the amount of data transferred across its science network creating workflows that cross facility boundaries [4]. This has increased the complexity of users successfully scheduling big data transfers. Hence, this has necessitated the demand for a tool that is generalizable, light weight, flexible and guarantees quality-of-services. In addition, a tool that shows a prior end-to-end throughput measurement that is attainable by an application using systems located at different sites alongside delivering other metrics relevant to the bulk data transfers and saving the results in a retentive memory.

The rest of the paper is organized as follows: Section 2 presents our proposed approach. Section 3 presents the description of Net-Preflight alongside it's implementation and use cases. Section 4 describes the experimental evaluation and discussion of results. Section 5 presents some past related work and finally, Section 6 presents conclusion and future work.

II. Our Approach

We choose an experimental approach for our comparison using a dedicated isolated cloud network testbed and a public internet network respectively. We conducted several experiments using different configurations like single, parallel and concurrent bulk data transfers between two endpoints. Building on the method reported in [1]. The objective is to measure the end-to-end bulk transfer throughput metrics. We upload large files with several file sizes to the destination node using the Secure File Transfer Protocol (SFTP) because it has the ability to leverage a secure connection to transfer files and traverse the file system on both the local and remote system. We then initiate concurrent downloads of the large files over and over again and record the total duration for the files to be downloaded from the destination node to the source node. With this time and known file sizes or bytes downloaded, we calculate a relative aggregated throughput graph over time. We then repeat the same set of experiments using different TCP variants, then take the measurements and observe the metrics and performance under different conditions. We then provide a throughput comparison measurement of some widely known TCP congestion control algorithms variants with different data transfer rates namely: TCP Reno [5], Hamilton TCP [6], Binary Increase Congestion control (BIC) [7] and Cubic [8]. We exposed our simulated network to a range of congestion conditions and compared multiple TCP congestion control algorithms in order to investigate the behavior of the alternate congestion control algorithms under little to modest congestion, which should reveal any differences in user experience when large files are sent over between sources and receivers with high-speed network interfaces. Different algorithms respond differently to network loads, but are based on the same principle to avoid congestion. So, we investigate the different congestion control algorithms that are included as loadable modules in the Linux kernel as reported in [9].

A. TCP Throughput Measurement and Socket buffersize using SFTP

We perform TCP throughput measurement utilizing and varying the socket buffersize and comparing it with default settings. We consider a unidirectional TCP data transfer from the source socket S_n to destination node D_n. TCP uses window-based flow control, such that source is allowed to have up to a certain number of transmitted unacknowledged bytes, called window size W_s. Then, W_c is the sender's congestion window and W_r is the receive window advertised by the source node S_n, and B_s is the size of the send socket buffer at source node S_n. The destination window W_r is amount of available receive socket buffer memory at source socket S_n, and is limited by source socket buffersize B_r.

Bottleneck Conditions: A link is said to be a bottleneck when the current bandwidth is less than the available bandwidth. Also, a link could be non-congested when its packet loss rate due to congestion is practically zero or when the current link capacity or bandwidth equals the available bandwidth. For simplicity, we used traffic shaping [10] bandwidth management technique to reduce the bandwidth of the link at both endpoints. We did not consider packet loss during our measurements hence it is out of scope. Equation (1) and (2) are used to calculate the measured throughput, where, T_p = Measured Throughput (mbps), B = Bytes downloaded, ΔT = t_n - t_s, t_n = current time, t_s = time started.

$$T_p = \frac{B}{\Delta T} = \frac{B}{t_n - t_s} \tag{1}$$

$$T_p(bps) = \frac{\text{WinSize(bits)}}{\text{Latency(sec)}} = \frac{\text{Bandwidth(bps)} * \text{RTT}}{\text{Latency(sec)}} \tag{2}$$

III. Net-Preflight Tool Description and Use Cases

In this section, we present Net-Preflight Tool Description and explored different use cases both on isolated networks and the public internet network path for DTN-to-DTN testing. Please note that the source code and implementation of Net-Preflight are available at [11].

A. Net-Preflight Tool Definition and End-to-End requirements

Net-PreFlight is a simple end-to-end, light-weight tool for measuring available throughput, traceroute. Compared to existing tools like Iperf, It saves all the previous results and configuration in its memory. It doesn't require root access at the destination node, which is one of the main contributions of our tool and makes it Unique. In addition, It mainly focuses on accurate throughput measurement, flexibility, a retentive memory, security, and performance-related issues.

 ISBN: 978-1-61208-895-2

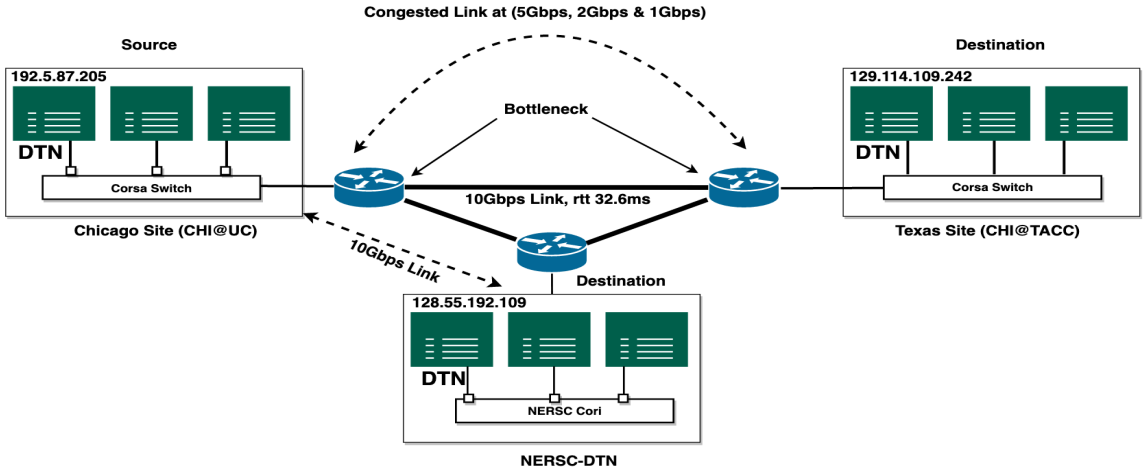

Fig. 1. Throughput measurement for large data transfer over isolated Network (CHI@UC to CHI@TACC) and public Network (NERSC DTN - CHI@UC DTN).

The main requirement of Net-Preflight is that you need to have a source and a destination IP, and both should be able to ping each other. Ideally, Net-Preflight was designed such that Root access is not required in both locations, but in this work, we have assumed we have files with different sizes saved in the destination node. To use the tool, you log in to your source node and run the command by specifying the required arguments, such as the destination IP address, the key file path, the target file, file size, and the number of iterations, respectively as stated in [11]. This operation initiates the download of the data from a destination to source over and over again as quickly as possible, then records how long it takes for the files to be downloaded alongside computing the difference. Using the time and known file size, a relative bandwidth graph is plotted over time, and the throughput is measured with respect to time.

B. Use Cases

1) Isolated Network (Network Setup between (CHI@UC to CHI@TACC): We present our first use case scenario, which is an isolated network over Chameleon testbed [12]. Chameleon is a large-scale, deeply re-configurable experimental platform, which is built to support Computer Sciences systems research with a wide variety of capabilities for researching systems, networking, distributed and cluster computing across multiple sites, such as the University of Chicago (CHI@UC) and Texas Computing Center (CHI@TACC), connected by a shared 100Gbps network. Figure 1 shows the network topology deployed on the isolated network over a dedicated 10Gbps bandwidth link. The goal of the experiment is download data from destination to source over and over again as quickly as possible, then record how long it takes for the files to be downloaded and compute the difference. Using the time and known file size, a relative bandwidth graph is plotted over time and the throughput is measured with respect to time.

2) Public Internet (Network Setup between (NERSC DTN - CHI@UC DTN): We present our second use case scenario experiment, which is a transfer from a DTN at the National Energy Research Scientific Computing Center (NERSC) to one of the nodes on the isolated network CHI@UC DTN. NERSC is a high performance computing (supercomputer) user facility operated by Lawrence Berkeley National Laboratory for the United States Department of Energy Office of Science. The DTN are NERSC servers dedicated to performing transfers between NERSC data storage resources such as HPSS and the NERSC Global File System (GFS), and storage resources at other sites. These nodes are being managed (and monitored for performance) as part of a collaborative effort between Energy Sciences Network (ESnet) and NERSC to enable high performance data movement over the high-bandwidth 100Gb ESnet wide-area network (WAN). All DTNs have two 100-gigabit ethernet links for outgoing connections and two 10-gigabit ethernet links to transfer to NERSC internal resources (HPSS). We repeat the same set of experiments similar to the isolated network scenario.

IV. EXPERIMENTAL EVALUATION

We conducted five experiments with respect to buffersize, file size, TCP congestion algorithm variant, limiting bandwidth and window size respectively.

A. ***Experiment 1*** - *Measurement w.r.t Buffersize and Filesize at 10Gbps link Capacity (Isolated network):*

This experiment was setup with the aim of evaluating the performance of the tool when data is transferred using different file sizes and buffersize. It was set-up on an isolated network using a 10Gbps link capacity between source and destination node. We performed the experiment varying the file transfer sizes between 5MB - 100MB along side using different buffersizes respectively.

B. ***Experiment 2*** - *Measurement w.r.t different TCP congestion algorithm with 10Gbps link Capacity(Isolated network):*

In this experiment, our aim was to evaluate the performance of the tool using different TCP congestion algorithm along side

 ISBN: 978-1-61208-895-2

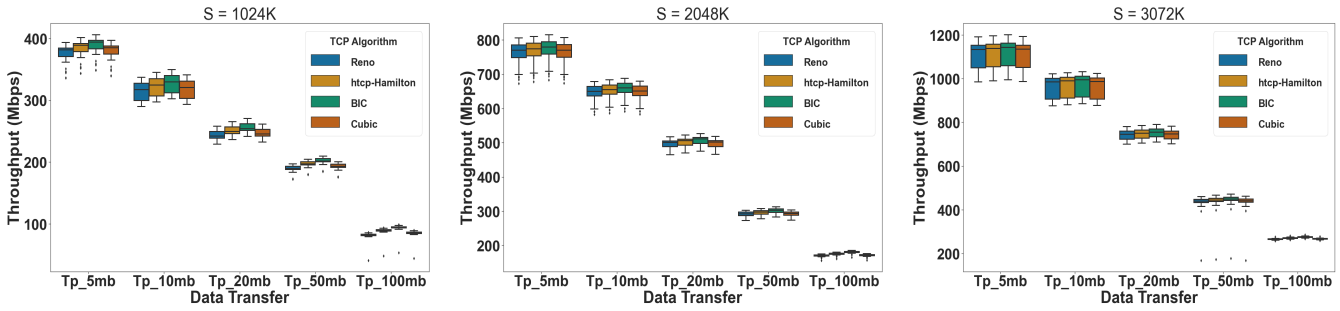

(a) (b) (c)

Fig. 2. Comparison of TCP congestion control algorithm comparison.

utilizing different file transfer sizes and buffersize. We started with Cubic, which is the current default TCP algorithm in most Linux operating systems, followed by Reno, Hamilton and BIC. The experiment was setup on an isolated network using a 10Gbps link capacity as shown in Figure 2.

C. ***Experiment 3*** - *Aggregated Throughput Measurement limiting bandwidth w.r.t congested vs Non-congested links (Isolated Network):*

In this experiment, we used the 10Gbps link capacity only. Several file transfers were tested at different congestion link capacity but keeping the buffersize constant. The aim was to introduce a bottleneck on the 10Gbps dedicated network link and observe the effect. The traffic at both source at destination node was limited using traffic shaping as reported in [10]. We start with the default link capacity of 10Gbps and then limit down to 5Gbps, 2Gbps and 1Gbps respectively as shown in Figure 3a.

D. ***Experiment 4*** - *Tool Comparison w.r.t Window size, Iperf vs Net-Preflight:*

Here, we tested measurements at window sizes from 8K - 1024k as shown in Figure 3b. We observed that there is a significant difference in network performance depending on the window size, with 128K window size being the most performed. This might be as result of the underlying background traffic condition, which resulted to a drop in throughput at 512K, 1024K and 2048K respectively.

E. ***Experiment 5*** - *Large file Aggregated Throughput Measurement w.r.t Concurrent transfers via Public Network from NERSC DTN - CHI@UC DTN:*

In this experiment, the aim was to evaluate the performance using huge concurrent file transfers with multiple streams (1, 2, 4, 6, and 8-Streams) with respect to 100MB, 200MB, 500MB 1GB and 2GB respectively (as shown in Figure 5). We show aggregated throughput keeping the buffersize constant and observing the effect of concurrent transfers on the aggregated throughput across a public network from NERSC DTN to CHI@UC DTN.

F. *Discussion of Results*

We collected throughput measurement for different data transfers sizes performed some experiments to observe the effect of different TCP congestion control variants on the throughput measurement. Figure 2 shows the comparison of various TCP congestion control algorithms. We conducted different experiments between buffersize S=512K and S=3072K while varying the data transfer files sizes between 5MB to 100MB, alongside comparing four TCP congestion control algorithm namely Reno, Hamilton, BIC, and Cubic, respectively. We observed that while keeping the buffersize constant at S=512K and S=1024K, a decrease in throughput was measured with increasing file size where BIC came out on top followed by Hamilton, BIC and Cubic. But as the buffersize increases between S=2048K and S=3072K, it was observed that it has less effect on the throughput measurement, which indicates that as we max out the buffersize, changes were not noticed between the TCP congestion control algorithms and hence becomes insensitive. However, on comparing all the four scenarios side-to-side, it was observed that an increase in the data transfer sizes results in a decrease in measured throughput while the opposite is true for the buffersize. But in all cases, BIC's performed best, followed by Hamilton and Cubic, then Reno.

Figure 3a shows a comparison of the congested link vs the non-congested link. We conducted this experiment in an isolated network between source node at Chicago and destination node and Texas. The default link capacity is 10Gbps, and several bulk file transfers were tested at different congestion link capacity but keeping the buffersize constant. The aim was to introduce some bottleneck on the network and observe the effect on the measure aggregated throughput. In order to introduce a bottleneck in the setup, the traffic at both source at destination node was limited using traffic shaping as reported in [10]. We started with the default link capacity of 10Gbps and then reduced it down to 5Gbps, 2Gbps, and 1Gbps, respectively. We observed that decreased in the link capacity result to a decrease in measure aggregated Throughput. A clear difference was observed in the measured throughput when the data transfer file was increased at different link capacities. The default link capacity of 10Gbps showed the highest throughput

 ISBN: 978-1-61208-895-2

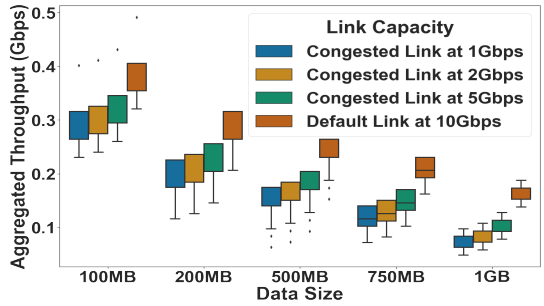

(a)

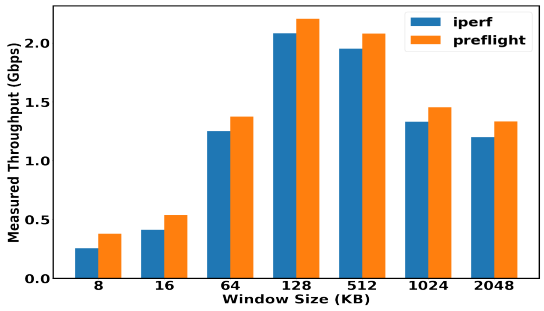

(b)

Fig. 3. (a)Testing Congestion Link vs non-congested links (b) Window Size Iperf vs Net-Preflight comparison.

while the 1Gbp congested link capacity showed the least aggregated throughput, which shows a good performance of Net-Preflight measurement tool.

Figure 3b shows the comparison between iperf vs Net-Preflight at different window sizes respectively. We further compared the performance of the throughput measurement between Iperf and Net-preflight as shown in Figure 4, where we kept the file transfer sizes between 20MB to 100MB. We observed that in both scenarios, while we keep the data transfer sizes constant, an increase in buffersize results to an increase in throughput. Overall Net-Preflight provided measurements largely in agreement with established tools. Figure 5 shows results of the experiments using large data transfers using concurrent and multiple streams of transfers. In this experiment, the aim was to evaluate the performance using huge concurrent file transfers of 100MB, 200MB, 500MB 1GB and 2GB, respectively. We performed the experiments over 30 iterations. We show aggregated throughput keeping the buffersize constant and observing the effect of concurrent transfers on the aggregated throughput. This time we started with a large buffersize S = 2048K. We kept the buffersize constant and varied the file transfer size starting from 100MB to 2GB. We then compare different streams of transfers from 1-stream to 8 streams respectively. It was observed that as we increase the file sizes the aggregated throughput increases, however a change is only noticed between the 1-stream and 2-streams. But, between 4-stream, 6-stream and 8-streams a significant change was not noticed. In addition, we also observed that an increase in buffersize from 2048k to 4096k corresponds to an increase in total aggregated throughput. *Why does Net-Preflight perform similar to Iperf?* Our results show a throughput measurement that is comparable to Iperf, which requires further exploration, since Net-Preflight also includes storage I/O in addtion to network characteristics. Upon further investigation, it is found that because Chameleon architecture has been optimized for I/O writes, hence we do not see it affecting the Net-Preflight results. Further analysis on a wide range of network infrastructure will be conducted in future.

V. Related Work

Past research has explored tools for network measurement, monitoring, available throughput estimation and bandwidth measurement [13]–[15], as well as analysis of TCP throughput and socket buffer auto-sizing for high-performance data transfers [16], [17]. The authors developed a simple analytic characterization of the steady state throughput as a function of loss rate and Round Trip Time(RTT) for a bulk transfers [2]. For instance the authors in [16] proposed a technique called SOBAS, their strategy was based on automatic socket buffer sizing at the application layer. Their results show that SOBAS provides consistently a significant throughput increase compared to TCP transfers that use the maximum possible socket buffersize. In a similar scenario, while the authors in [18] analyzes the Incast problem, the authors in [19] examined the effects of using parallel TCP flows to improve end-to-end network performance for distributed data intensive applications. While the authors in [20] describes the analysis of TCP/IP socket buffer length in Local Area Network (LAN) and Wide Area Network (WAN), authors in [21] presented a MPT-GRE software, which is a two multipath communication systems based on different technologies. Following from various traditional approaches, a lot of existing network monitoring tools lack the capability of retaining all previous measurements, flexibility and security in terms of having root access to both ends. Hence this paper propose Net-Preflight, a tool intended to bridge the gap by indicating the state of the network between two nodes in an overlay, prior to initiating large data transfers.

VI. Conclusion and Future Work

This paper presents Net-Preflight, a tool intended to indicate the state of the network between two nodes in an overlay, prior to performing large scale data transfers. It was compared with existing tools using different metrics and utilizing isolated networks, like Chameleon testbed and public internet transfers. The comparison focused on throughput accuracy, flexibility and performance history, which stores previous configurations and network measurements. Net-Preflight addresses questions of how concurrent stream connections can improve aggregate TCP throughput measurement. It also addresses the question of how to select the maximum number of sockets necessary to maximize TCP throughput while simultaneously avoiding congestion. Our results show that the use of parallel TCP streams is equivalent to using a large maximum segment size on a single connection. In the future, we will continue to

 ISBN: 978-1-61208-895-2

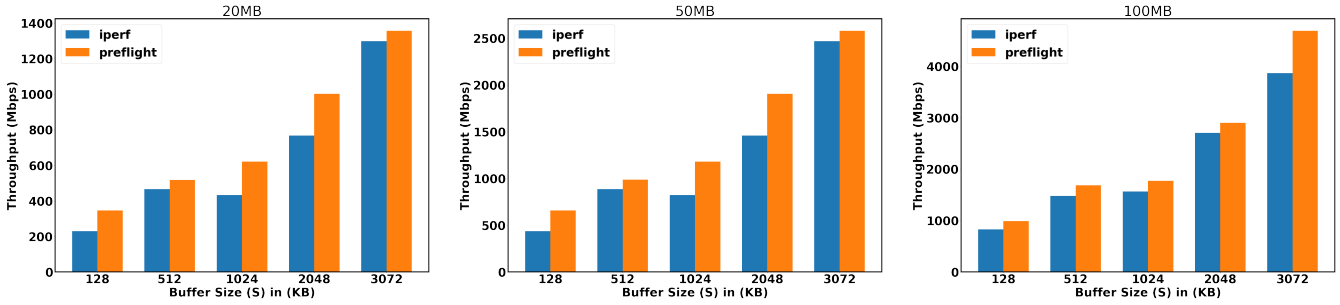

Fig. 4. Iperf and Net-Preflight data transfer comparison.

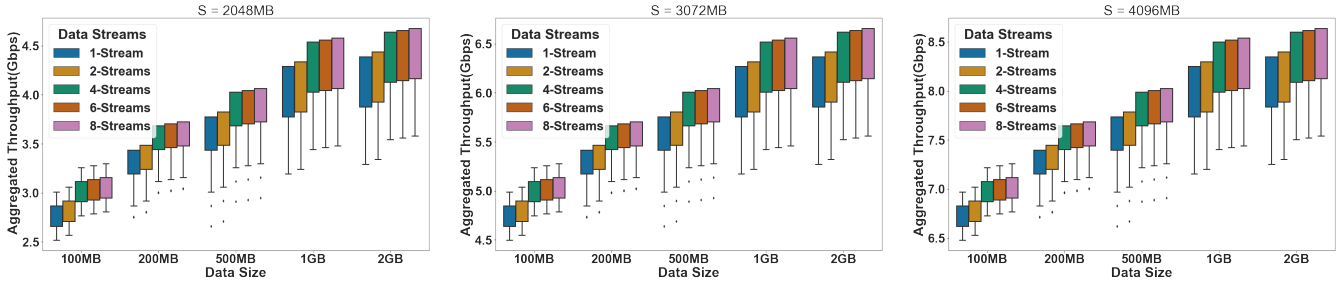

Fig. 5. Large file concurrent transfers.

improve the performance of the tool and explore the possibility of applying learning techniques to predict the future end-to-end throughput and latency that is attainable by the tool.

REFERENCES

[1] M. Allman, "Measuring end-to-end bulk transfer capacity," in *Proceedings of the 1st ACM SIGCOMM Workshop on Internet Measurement*, pp. 139–143, 2001.

[2] J. Padhye, V. Firoiu, D. Towsley, and J. Kurose, "Modeling tcp throughput: A simple model and its empirical validation," in *Proceedings of the ACM SIGCOMM'98 conference on Applications, technologies, architectures, and protocols for computer communication*, pp. 303–314, 1998.

[3] J. Zurawski *et al.*, "perfsonar: On-board diagnostics for big data," in *1st Workshop on Big Data and Science*, pp. 1–6, Citeseer, 2013.

[4] B. Enders, D. Bard, C. Snavely, L. Gerhardt, J. Lee, B. Totzke, K. Antypas, S. Byna, R. Cheema, S. Cholia, M. Day, A. Gaur, A. Greiner, T. Groves, M. Kiran, Q. Koziol, K. Rowland, C. Samuel, A. Selvarajan, A. Sim, D. Skinner, R. Thomas, and G. Torok, "Cross-facility science with the superfacility project at lbnl," in *2020 IEEE/ACM 2nd Annual Workshop on Extreme-scale Experiment-in-the-Loop Computing (XLOOP)*, pp. 1–7, 2020.

[5] Y. Nishida, "The newreno modification to tcp's fast recovery algorithm," *Standards Track, PP*, pp. 1–16, 2012.

[6] D. Leith and R. Shorten, "H-tcp: Tcp for high-speed and long-distance networks," in *Proceedings of PFLDnet*, vol. 2004, pp. 1–6, 2004.

[7] L. Xu, K. Harfoush, and I. Rhee, "Binary increase congestion control (bic) for fast long-distance networks," in *IEEE INFOCOM 2004*, vol. 4, pp. 2514–2524, IEEE, 2004.

[8] S. Ha and I. Rhee, "Taming the elephants: New tcp slow start," *Computer Networks*, vol. 55, no. 9, pp. 2092–2110, 2011.

[9] A. Esterhuizen and A. Krzesinski, "Tcp congestion control comparison," *SATNAC, September*, pp. 1–6, 2012.

[10] P. Kanuparthy and C. Dovrolis, "Shaperprobe: end-to-end detection of isp traffic shaping using active methods," in *Proceedings of the 2011 ACM SIGCOMM conference on Internet measurement conference*, pp. 473–482, 2011.

[11] B. Mohammed, M. Kiran, and B. Enders, "Net-Preflight Github repository: https://github.com/esnet/netpreflight-performancetest." Accessed: 2021-09-26.

[12] K. Keahey *et al.*, "Lessons learned from the chameleon testbed," in *Proceedings of the 2020 USENIX Annual Technical Conference (USENIX ATC '20)*, USENIX Association, July 2020.

[13] J. Strauss, D. Katabi, and F. Kaashoek, "A measurement study of available bandwidth estimation tools," in *Proceedings of the 3rd ACM SIGCOMM conference on Internet measurement*, pp. 39–44, 2003.

[14] A. Tirumala, L. Cottrell, and T. Dunigan, "Measuring end-to-end bandwidth with iperf using web100," in *In Web100, Proc. of Passive and Active Measurement Workshop*, Citeseer, 2003.

[15] D. Kaur, B. Mohammed, and M. Kiran, "Netgraf: A collaborative network monitoring stack for network experimental testbeds," *arXiv preprint arXiv:2105.10326*, 2021.

[16] R. S. Prasad, M. Jain, and C. Dovrolis, "Socket buffer auto-sizing for high-performance data transfers," *Journal of GRID computing*, vol. 1, no. 4, pp. 361–376, 2003.

[17] M. Jain, R. S. Prasad, and C. Dovrolis, "The tcp bandwidth-delay product revisited: network buffering, cross traffic, and socket buffer auto-sizing," tech. rep., Georgia Institute of Technology, 2003.

[18] A. Phanishayee, E. Krevat, V. Vasudevan, D. G. Andersen, G. R. Ganger, G. A. Gibson, and S. Seshan, "Measurement and analysis of tcp throughput collapse in cluster-based storage systems.," in *FAST*, vol. 8, pp. 1–14, 2008.

[19] T. J. Hacker, B. D. Athey, and B. Noble, "The end-to-end performance effects of parallel tcp sockets on a lossy wide-area network," in *Proceedings 16th International Parallel and Distributed Processing Symposium*, pp. 10–pp, IEEE, 2002.

[20] L. Mazalan, S. S. S. Hamdan, N. Masudi, H. Hashim, R. Abd Rahman, N. M. Tahir, N. M. Zaini, R. Rosli, and H. A. Omar, "Throughput analysis of lan and wan network based on socket buffer length using jperf," in *2013 IEEE International Conference on Control System, Computing and Engineering*, pp. 621–625, IEEE, 2013.

[21] S. Szilágyi, F. Fejes, and R. Katona, "Throughput performance comparison of mpt-gre and mptcp in the fast ethernet ipv4/ipv6 environment," *Journal of Telecommunications and Information Technology*, 2018.

 ISBN: 978-1-61208-895-2

Breach-Free Scheduling of Reinforced Sensor Barriers

Jorge A. Cobb
Department of Computer Science
The University of Texas at Dallas
Richardson, TX 75080-3021
U.S.A.
Email: cobb@utdallas.edu

***Abstract*—Intrusion detection is an important function of wireless sensor networks. Due to their limited lifetime, rather than covering the entire area of interest at all times, sensors can be divided into barriers, where each barrier is a subset of sensors that prevents the intruder from crossing the area. However, a security problem was discovered, known as a *barrier-breach*, where an intruder can find a location in between two consecutive barriers that allows the area to be crossed when one barrier is replaced by the next. Given a set of barriers, deciding if there is a breach-free schedule of these barriers is intractable. This has led to the development of several heuristics. In a recent work, we introduced *reinforced* sensor barriers, which prevent the crossing of the area of interest in more than one direction, and presented heuristics for obtaining the maximum number of reinforced barriers. However, this work did not address obtaining a breach-free schedule for these barriers. In this paper, we present a heuristic to obtain a breach-free schedule of reinforced barriers from a random placement of sensors in the area of interest. We show via simulation that in practical scenarios the heuristic achieves a schedule that is close to optimal.**

***Index Terms*—sensor networks; barrier coverage; security breaches**

I. Introduction

A Wireless Sensor Network (WSN) consists of an area of interest in which sensor nodes have been randomly placed. Due to running on batteries, sensors have a limited lifetime [1]. One important use of a WSN is intrusion detection, in which sensors monitor the area of interest and report to a base station any anomalous presence. Typically, sensors have a sensing range that is significantly smaller that the area of interest, and thus, multiple sensors need to be operating simultaneously.

Due to their limited lifetime, it is common to have more sensors than necessary to cover the area. Sensors are divided into groups, where each group covers the entire area. A sleep-wakeup schedule is created, where one sensor group is active and the remaining are asleep. Once the first group's battery is close to exhaustion, the second group is activated, and so on.

The degree to which the area of interest is covered by active sensors falls in two categories: full coverage and partial coverage. In full coverage, the entire area is covered at all times by the active sensors [2]–[5]. In partial coverage, only certain regions are covered at a time by the active sensors. Thus, any event occurring outside of covered area is not detected [6]–[8].

A particular form of partial coverage is *barrier coverage*, where each group of sensors forms a barrier across the area such that intruders are prevented from crossing undetected. There have been extensive studies of sensor barriers due to their many applications [9]–[16]. Fig. 1(a) highlights a subset of sensors that provide barrier coverage to the area. The highlighted sensors will remain active and the rest asleep until they are close to exhausting their battery power. If n disjoint barriers are constructed, the protection lasts n times the lifetime of a sensor. Fig. 1(b) shows the sensors divided into four disjoint barriers.

The problem of dividing the sensors into the maximum number of disjoint barriers has been solved in polynomial time [11]. The approach is based on transforming the sensor connectivity graph into a maximum flow problem.

Subsequently, a vulnerability of sensor barriers, known as a *barrier breach*, was discovered [17], [18]. For some barriers, it is possible for an intruder to cross the area of interest after activating one barrier and deactivating the previous one.

Fig. 1(b) illustrates barrier breaches. Four different sensor barriers are displayed with different line types. If we use the barriers in a sequential sleep-wakeup cycle (B_1, B_2, B_3, and finally B_4), the users are protected for a total of four time units. However, the order in which the barriers are scheduled affects the effectiveness of the barriers. Instead, consider scheduling B_2 followed by B_1. In this case, an intruder could move to the point highlighted by a diamond, and after B_2 is turned off, the intruder is free to cross the area. Also, note that only one of B_3 or B_4 is of use. If we activate B_3 first, then the intruder can move to the location marked by the black star. When B_4 is activated and B_3 deactivated, the intruder can reach the users undetected. The situation is similar if B_4 is activated first, and the intruder moves to the location of the grey star.

There have been several heuristics that generate a set of sensors barriers and their breach-free schedule from randomly placed sensors [17]–[20]. In [21], it is shown that, *given* a set of disjoint barriers, obtaining the longest breach-free schedule of the given barriers is intractable, and a probabilistic algorithm is given for the problem. The complexity of finding the longest breach-free schedule of barriers from a from a random placement of nodes remains an open problem.

A stronger form of a barrier, called a *reinforced barrier*, was

 ISBN: 978-1-61208-895-2

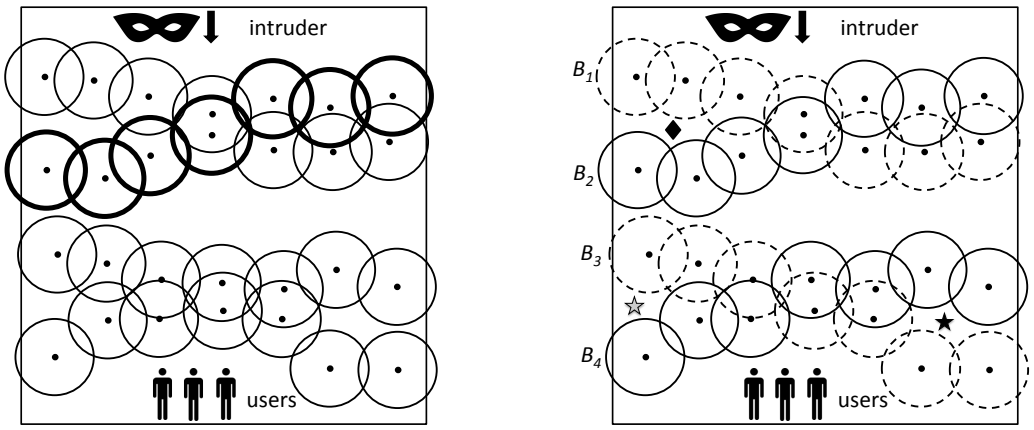

(a) Sensor Barrier (b) Barrier Breaches

Fig. 1. Sensor Barriers

introduced in our earlier work [22]. To illustrate this barrier, consider Fig. 2(a), in which the area of interest is a rectangle. The objective is to prevent an intruder from crossing the area by entering from any of its sides and exiting via another side. For example, intrusion I_1 is a vertical intrusion, intrusion I_2 is a horizontal intrusion, while I_3 is a corner intrusion (by turning from vertical to horizontal).

To prevent these intrusions, consider Fig. 2(b), where there is a barrier of sensors from corner U_1 to corner V_1, and another barrier from corner U_2 to corner V_2. Notice that these two barriers do not need to be disjoint. By combining these two barriers, none of the above intrusions are possible.

Heuristics to obtain the maximum number of reinforced barriers were presented in [22]. However, the issue of barrier breaches was not addressed. Note that barrier breaches are still possible, as shown in Fig. 2(c). The figure consists of two reinforced barriers drawn with different line styles. If we schedule the solid line barrier first, then an intruder can arrive from the top side. Once we switch to the dashed-line barrier, the intruder is free to exit via the right side. The issue is similar if we schedule the dashed barrier first.

In this paper, we consider the problem of obtaining a maximum-length breach-free schedule of reinforced barriers starting from a random placement of sensor nodes. We present a parameterized algorithm based on the general approach presented in [21]. The algorithm is exponential in the number of barriers, which is expected to be small and is polynomial in the number of sensor nodes. Via simulation we demonstrate that the method produces schedules of near-optimal length.

The rest of this paper is organized as follows. Section II presents background and definitions. In Section III, we present our heuristic. Simulation results are presented in Section IV. Concluding remarks are given in Section V.

II. BACKGROUND

In this section, we present definitions and discuss earlier methods, before we present our heuristic in Section III.

A. Definitions

We consider a rectangular area where a set S of n sensor nodes have been deployed randomly. A *barrier* consists of a set B, $B \subseteq S$, such that there is a sequence of sensors, $s_1, s_2, \ldots, s_k$, such that the sensor ranges of s_i and s_{i+1}, $1 \leq i < k$, overlap with each other, and furthermore, the sensing range of s_1 overlaps one of the sides of the rectangle, while the sensing range of s_k overlaps the opposite side of the rectangle. Barrier B_1 in Fig. 1(b) is an example. A barrier is vertical if the sides being overlapped are the top and bottom, and is horizontal otherwise.

A *reinforced barrier* R is a set of sensors such that a line cannot be drawn starting from a side of the rectangle and ending at a different side without crossing the sensing area of any one of the sensors. Note that this requires the corners to be covered, and it also implies that there is a subset R' of R such that R acts both as a horizontal and vertical barrier (i.e., a diagonal barrier). By symmetry, R is the union of two diagonal barriers.

An ordered pair (B_1, B_2) of horizontal barriers forms a *breach* if there is a point p not covered by either barrier such that a line can be drawn from the top of the area to p without overlapping the sensing area of B_1, and furthermore, a line can be from p to the bottom of the area without overlapping the sensing area of B_2. A sequence (or schedule) of barriers $B_1, B_2, \ldots, B_k$ is *breach-free* if every pair of consecutive barriers in the sequence does not form a breach.

Similarly, an unordered pair (R_1, R_2) of reinforced barriers forms a breach if there is a point p not covered by either barrier such that a line can be drawn from some side of the area to p without overlapping R_1, and furthermore, a line can be drawn to p to a *different* side of the area without overlapping R_2.

B. Longest Barrier Schedule

Finding the largest number of horizontal disjoint barriers has been solved in polynomial time by Kumar et al. [11] with their algorithm known as Stint. The method builds a flow graph F where the maximum flow corresponds to the number of

 ISBN: 978-1-61208-895-2

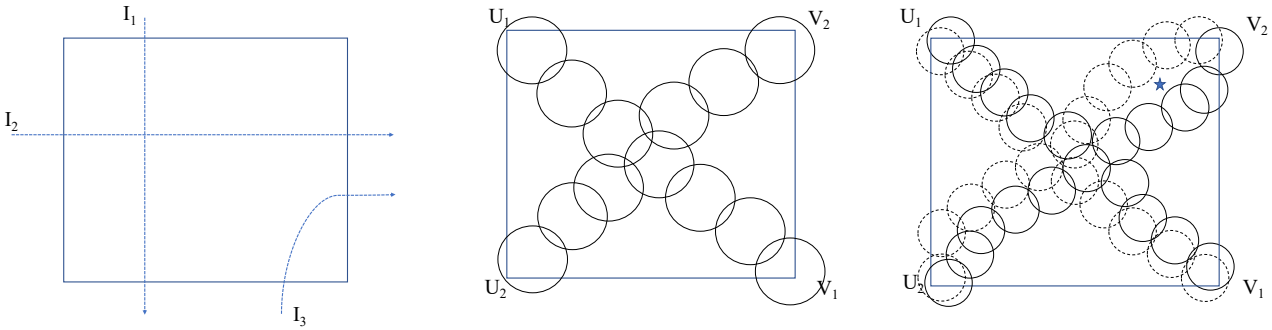

(a) Area Intrusions (b) Reinforced Barrier (c) Reinforced Barrier Breach

Fig. 2. Reinforced Sensor Barriers

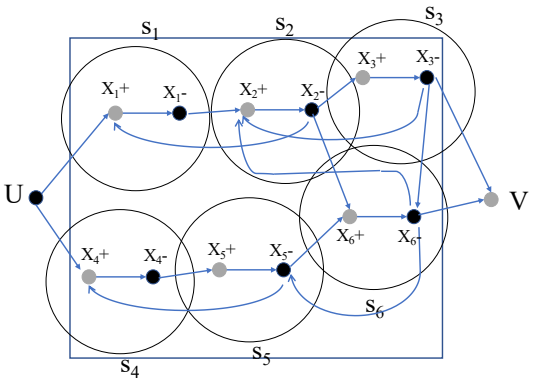

Fig. 3. Stint Maximum Flow Method

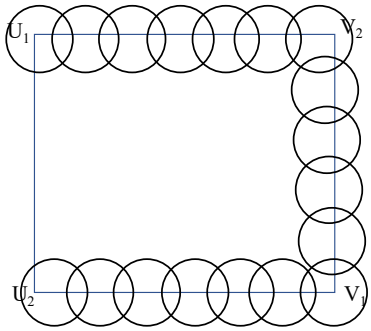

Fig. 4. Reinforced Barrier Extreme Case

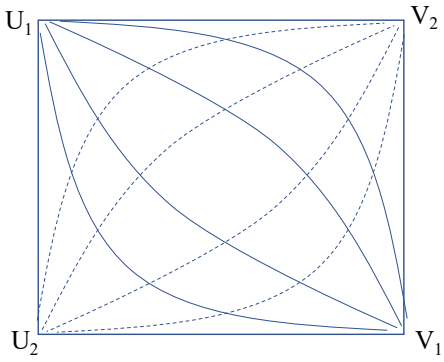

Fig. 5. Diagonal Barriers

sensor barriers, and a path with non-zero flow corresponds to a barrier. A brief outline of the method is as follows, and a sample graph F is illustrated in Fig. 3.

Create two nodes U and V representing the left and the right borders, respectively. Then, for each sensor node s_i, create two nodes, x_i+ and x_i-, with a directed edge (x_i+, x_i-) of capacity one. This edge corresponds to the life of the sensor. All other edges have a capacity of infinity. For every sensor s_i overlapping the left border, add the directed edge (U, x_i+), and for every sensor s_j overlapping the right border, add the directed edge (x_j-, V). Finally, for every pair of sensors s_i and s_j whose sensing area overlaps, add an edge (x_i-, x_j+) and (x_j-, x_i+).

It is easy to show that a barrier-cover corresponds to a path from U to V in F. Since the capacities are integers, the maximum flow f in F is an integer, which corresponds to f edge-disjoint paths, and thus f node-disjoint barriers.

Most heuristics, such as [17], [18], create their schedule of barriers by first obtaining a set of barriers from the Stint algorithm, followed by selecting a subset of these barriers that do not cross each other. Another approach [21] is to simply try all possible schedules obtained from the Stint barriers. If the longest schedule is of length l, then the approach is exponential in l, but polynomial in the number of sensor nodes. Due to this exponential growth, a probabilistic algorithm was presented in [21] that finds the longest schedule with high probability.

Note that the barriers chosen for the above methods are obtained from the output of Stint. There is, however, no guarantee that the set of barriers that can generate the longest possible schedule are the barriers obtained from Stint.

III. Breach-Free Reinforced Stint Barriers

In this section, we present our heuristic for obtaining the longest breach-free schedule of reinforced barriers. As shown

in Fig. 2(b), two diagonal barriers are needed to form a reinforced barrier. Note that this is always the case even when the diagonal barriers are not apparent. Consider for example Fig. 4 where there is a sequence of sensor nodes covering all three sides $\overline{U_1V_2}$, $\overline{V_2V_1}$, and $\overline{V_1U_2}$. Given that the diagonal barriers do not need to be disjoint (they will be activated concurrently), then this sequence of nodes can be thought of as two diagonal barriers, the first from U_1 to V_1 along sides $\overline{U_1V_2}$ and $\overline{V_2V_1}$, and the second from U_2 to V_2 along sides $\overline{U_2V_1}$ and $\overline{V_1V_2}$.

Our approach consists in first obtaining the maximum number of disjoint diagonal barriers from U_1 to V_1, and then combining them with the maximum number of disjoint barriers from U_2 to V_2. This is illustrated in Fig. 5. Let $\mathcal{D}_1 = \{B_{1,1}, B_{1,2}, B_{1,m_1}\}$, where $|\mathcal{D}_1| = m_1$, be a maximal set of disjoint barriers from U_1 to V_1. Similarly, let $\mathcal{D}_2 = \{B_{2,1}, B_{2,2}, B_{2,m_2}\}$, $|\mathcal{D}_2| = m_2$, be a maximal set of disjoint barriers from U_2 to V_2. Then, the union of any two barriers $B_{1,i}$ and $B_{2,j}$, where $B_{1,i} \in \mathcal{D}_1$ and $B_{2,j} \in \mathcal{D}_2$, form a reinforced barrier, $R_{i,j}$. Note in particular that $B_{1,i}$ and $B_{2,j}$ do not need to be disjoint since they will be activated simultaneously. We denote the set of all reinforced barriers with $\mathcal{R}$, i.e., $\mathcal{R} = \bigcup_{i,j} R_{i,j}$.

To obtain the set of barriers $\mathcal{D}_1$ and $\mathcal{D}_2$ we can take advantage of Stint by running it twice: the first time to obtain $\mathcal{D}_1$ and the second time to obtain $\mathcal{D}_2$. To obtain $\mathcal{D}_1$, the flow graph F_1 is built with an arc from U_1 to each node x_i+, where s_i is a sensor whose sensing are overlaps U_1's corner. Also, an arc is made from each x_j- to V_1, where the sensor area of x_j overlaps V_1's corner. The arcs between sensor nodes are the same as before. A similar approach using U_2 and V_2 will yield the set $\mathcal{D}_2$.

Our objective is to find the maximum breach-free schedule using the reinforced barriers in $\mathcal{R}$. To accomplish this, we build a graph G whose nodes are elements of $\mathcal{R}$. An edge exists from an element $R_{i,j}$ to an element $R_{k,l}$ if the pair $(R_{i,j}, R_{k,l})$ does not constitute a breach. Obtaining the longest breach-free schedule is equivalent to the problem of finding the longest path in G starting at an arbitrary node and without repeating nodes in the path.

The above approach is similar to the one used in [21], except that the problem considered is obtaining a maximum breach-free schedule of horizontal barriers. The barriers are obtained from Stint, and a graph is built such that an arc corresponds to a pair of horizontal barriers that do not form a breach.

There is a significant difference in the case of reinforced barriers that does not occur in horizontal barriers. That is, reinforced barriers are not independent of each other. If a barrier $R_{i,j}$ is used somewhere in the schedule, then for any i, $R_{i,l}$ cannot appear in the same schedule. This is because the diagonal barrier $B_i \in \mathcal{D}_i$ takes part in both reinforced barriers $R_{i,j}$ and $R_{i,l}$, and barrier B_i can only appear once in a schedule. We refer to the pair $R_{i,j}$ and $R_{i,l}$ as being *incompatible* barriers. Similarly, barrier $R_{i,j}$ is incompatible with barriers $R_{k,j}$ for all k.

Note that, because incompatible barriers cannot appear in a schedule, then the length of the schedule is upper bounded by $\min(|\mathcal{D}_1|, |\mathcal{D}_2|)$, i.e., $\min(m_1, m_2)$. Without this restriction, the length of the schedule could be as large as $m_1 \cdot m_2$.

This restriction on the length of the schedule is of significant consequence, because finding the longest path in a graph is an NP-Complete problem. A parameterized algorithm on the length l of the schedule can be obtained using dynamic programming combined with exploring all possible subsets of the set of barriers [21], and hence, it is exponential in the number of barriers. Since l is bounded by the number of barriers, the running time is significant for nontrivial problems. This motivated the authors of [21] to present a more efficient but probabilistic algorithm.

On the other hand, with reinforced barriers, the longest path of the graph is bounded by $\min(m_1, m_2)$, which yields a significantly smaller number. In addition, a diagonal barrier must begin with a sensor whose area overlaps a corner, while for horizontal barriers any sensor overlapping a side border can be used as a starting point. Therefore, we leave the possibility of a probabilistic algorithm for future work, and we consider all possible paths of length at most $\min(m_1, m_2)$.

As a final remark, the barriers obtained from Stint are not guaranteed to be the set of barriers from which an optimal schedule is obtained. Nonetheless, $\min(m_1, m_2)$ is an upper bound on the length of a breach-free schedule of reinforced barriers. The complete method is shown in Algorithm 1.

IV. Simulation Results

In this section, we compare the performance of the Breach-Free Reinforced Barriers (BFRB) algorithm against two upper bounds. Our objective is to determine how close our algorithm is in obtaining an optimal solution.

Our algorithm is compared against the Minimum Intervention Paths (MIP) heuristic [22]. This is a heuristic we presented for the problem of finding the maximum number of reinforced barriers. Since it does not take barrier breaches into account, we expect it to yield longer schedules than those of our BFRB algorithm. MIP is based on a greedy strategy that chooses a pair of diagonal barriers from $\mathcal{D}_1$ and $\mathcal{D}_2$ that overlap the least number of other barriers. In this way, a greater number of barriers are available for the subsequent round of the algorithm. Our algorithm is also compared against the upper bound m, where $m = \min(|\mathcal{D}_1|, |\mathcal{D}_2|)$. It is impossible to obtain a schedule longer than m, regarldess of whether breaches are present or not.

The area of interest is a square of size 500×500 meters. We also simulated a rectangular area of dimension 400×600 meters. Sensor nodes are randomly deployed in each area, ranging from 100 to 260. In addition, the radius of the sensing area for sensors ranges from 60 to 130. Every point in our plots corresponds to the average of 100 simulations.

Fig. 6 plots the sensor radius vs. the resulting reinforced breach-free schedule length. The number of sensors is maintained constant at 250. As the radius increases, the diagonal barrier sets $\mathcal{D}_1$ and $\mathcal{D}_2$ increase in size, and therefore, so does the total number of reinforced barriers from which a schedule

 ISBN: 978-1-61208-895-2

Algorithm 1 ***Breach-Free Reinforced Barriers***
Inputs: sensor set S and rectangular area A.
Output: breach-free schedule of reinforced barriers.

$(U_1, V_2, V_1, U_2) \leftarrow$ the four clockwise corners of A.
$F \leftarrow (V_F, E_F)$; // (flow graph)
$V_F \leftarrow \{U_1, V_1\}$; $E_F \leftarrow \emptyset$;
for each s, $s \in S$, **do**
  $V_F \leftarrow V_F \cup \{x_s+, x_s-\}$; $E_F \leftarrow E_F \cup \{(x_s+, x_s-, 1)\}$;
  $E_F \leftarrow E_F \cup \{(U_1, x_s+, \infty)\}$ if $U_1 \in$ *sensing_area*(s);
  $E_F \leftarrow E_F \cup \{(x_s-, V_1, \infty)\}$ if $V_1 \in$ *sensing_area*(s);
  for each s', $s' \in S \wedge s \neq s' \wedge$ *overlapping_sensing_area*(s, s'), **do**
    $E_F \leftarrow E_F \cup \{(x_s+, x'_s-, \infty)\} \cup \{(x'_s+, x_s-, \infty)\}$;
  end for
end for
$F' \leftarrow$ *Ford-Fulkerson-Max-Flow*(F);
$\mathcal{D}_1 \leftarrow \langle\rangle$; // empty sequence of diagonal barriers)
for each path P in F' with non-zero capacity **do**
  $\mathcal{D}_1 \leftarrow \mathcal{D}_1 : barrier(P)$; // add the barrier
                // corresponding to path P
end for
$m_1 \leftarrow |\mathcal{D}_1|$;
Obtain similarly $\mathcal{D}_2$ from U_2 and V_2;
$m_2 \leftarrow |\mathcal{D}_2|$;
$m \leftarrow$ *min*(m_1, m_2);
for each i and j, $1 \leq i \leq m_1 \wedge 1 \leq j \leq m_2$, **do**
  $R_{i,j} \leftarrow \mathcal{D}_1(i) \cup \mathcal{D}_2(j)$;
end for
$G \leftarrow (V_G, E_G)$; // (breach graph)
for each i and j, $1 \leq i \leq m_1 \wedge 1 \leq j \leq m_2$, **do**
  $V_G \leftarrow V_G \cup \{R_{i,j}\}$;
end for
for each i, j, k, l, $1 \leq i, k \leq m_1 \wedge 1 \leq j, l \leq m_2$, **do**
  $E_G \leftarrow E_G \cup \{(R_{i,j}, R_{k,l})\}$
            if $(R_{i,j}, R_{k,l})$ is not breached;
end for
$Q \leftarrow$ longest path (length at most m) in G.
return Q

can be obtained. Note that BRFB remains significantly close the the upper bound of m, and therefore, the breach-free schedule lengths found are close to the maximum possible schedule (breach-free or not).

We observe that our MIP heuristic, which is oblivious to breaches, produces the longest possible schedules. We have no formal results on the optimality of MIP, and it is unlikely optimal, but from this performance it deserves further study.

Figure 7 plots the number of sensors vs. the resulting reinforced breach-free schedule length. The sensor radius is maintained at 90. The results are similar to those of the previous figure. BRFB obtains schedules that are close in length to those of the strict upper bound.

It is worth noticing that the number of schedules obtained is relatively small. This is related to the fact that for a diagonal

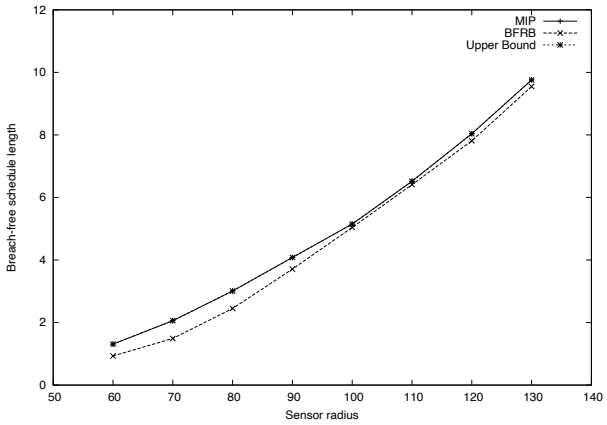

Fig. 6. Radius vs. schedule length in square area.

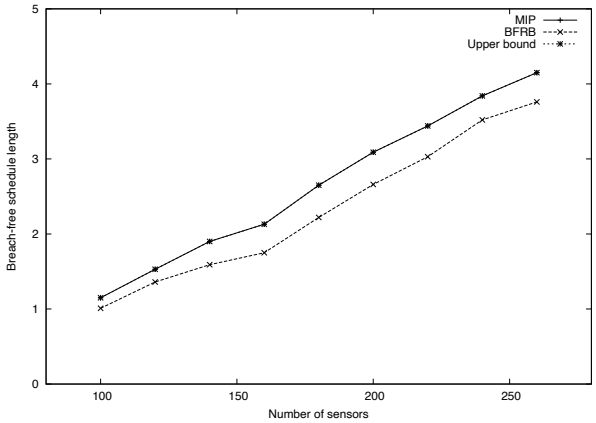

Fig. 7. Number of sensors vs schedule length in square area.

barrier to exist, there has to be a sensor covering each of the corners of the area. Given the random placement of sensors, the number of sensors in these positions are few. In addition, due to the upper bound m, which is the minimum of the two sets of diagonal barriers, we expect the total number of reinforced barriers (breach-free or not) to be small.

Fig. 8 and Fig. 9 are similar to Fig. 6 and Fig. 7, except that the area is now a 400×600 rectangle. As before, BRFB obtains schedules that are close in length to those of the strict upper bound.

V. Concluding Remarks and Future Work

We presented a heuristic for the reinforced breach-free barriers problem, and we have shown that it performs well, achieving schedule lengths close to the upper bound. The heuristic suffers from the drawback that all schedules of length m obtained from $\mathcal{R}$ have to be examined. Note that $|\mathcal{R}| = m_1 \cdot m_2$, so a relatively small number of barriers, say, $\mathcal{D}_1 = \mathcal{D}_2 = 10$, yields a significantly number of possible reinforced barriers, $|R| = 100$.

We considered two approaches to examine all schedules. The first is to use a dynamic programming technique similar to that in [21], where, for every possible subset of $\mathcal{R}$, a value

 ISBN: 978-1-61208-895-2

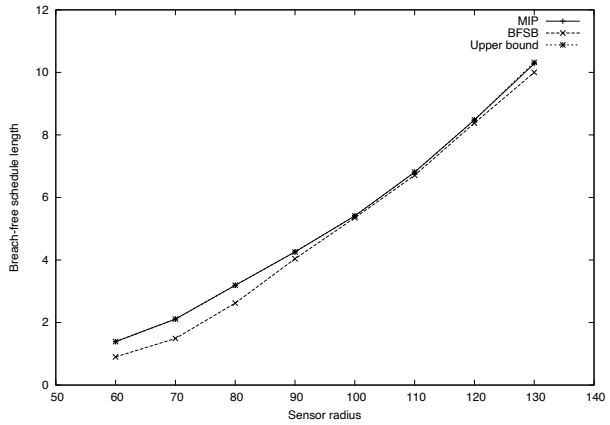

Fig. 8. Radius vs. schedule length in rectangular area.

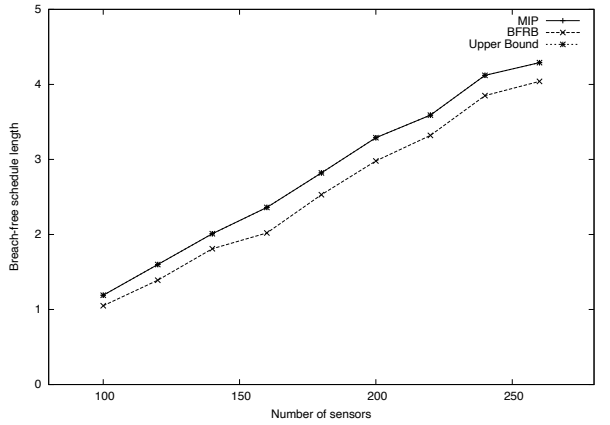

Fig. 9. Number of sensors vs schedule length in rectangular area.

(the length of the longest schedule using the subset) needs to be maintained. Above, this would require 2^{100} values.

The second approach, which we adopted, is to take advantage of the small value of m, and build all possible schedules of length m, ensuring that each addition to the schedule is in agreement with the breach-free graph G, and furthermore, that any new barrier added to the schedule is not incompatible with earlier barriers in the schedule. Nonetheless, in the worst case, the number of steps required is $|\mathcal{R}|^m$, which becomes infeasible as m grows. Given the above difficulties, we will explore probabilistic algorithms in the future and compare their performance against the known upper bound.

Finally, in earlier work on breach-free horizontal barriers, we developed algorithms that do not use the Stint method as a source of barriers, but rather developed barriers in a top-down approach ensuring that each new barrier does not create a breach with earlier barriers [19] [20]. A similar approach might be possible for the case of reinforced barriers, but barriers would have to be constructed in parallel over all sides. We will also leave this approach for future work.

REFERENCES

[1] I. F. Akyildiz, W. Su, Y. Sankarasubramaniam, and E. Cayirci, "Wireless sensor networks: a survey," Computer Networks, vol. 38, no. 4, March 2002, pp. 393–422.

[2] C. Huang and Y. Tseng, "The coverage problem in a wireless sensor network," in ACM Int'l Workshop on Wireless Sensor Networks and Applications (WSNA), 2003.

[3] H. Zhang and J. Hou, "On deriving the upper bound of α-lifetime for large sensor networks," in Proc. of The 5th ACM Int'l Symposium on Mobile Ad-hoc Networking and Computing (MobiHoc), 2004.

[4] Cardei, M., Thai, M.T., Y. Li, and W. Wu, "Energy-efficient target coverage in wireless sensor networks," in INFOCOM, 24th Annual Joint Conf. of the IEEE Computer and Comm. Societies, vol. 3, March 2005.

[5] M. Thai, Y. Li, and F. Wang, "O(log n)-localized algorithms on the coverage problem in heterogeneous sensor networks," in IEEE Int'l Performance, Computing, and Comm. Conference, IPCCC, April 2007, pp. 85–92.

[6] S. Gao, X. Wang, and Y. Li, "p-percent coverage schedule in wireless sensor networks," in Proc. of 17th Int'l Conference on Computer Communications and Networks, ICCCN, August 2008, pp. 1–6.

[7] C. Vu, G. Chen, Y. Zhao, and Y. Li, "A universal framework for partial coverage in wireless sensor networks," in IEEE 28th Int'l Perf. Computing and Comm. Conf. (IPCCC), December 2009, pp. 1–8.

[8] Y. Li, C. Vu, C. Ai, G. Chen, and Y. Zhao, "Transforming complete coverage algorithms to partial coverage algorithms for wireless sensor networks," IEEE Transactions on Parallel and Distributed Systems, vol. 22, no. 4, April 2011.

[9] S. Kumar, T. Lai, and A. Arora, "Barrier coverage with wireless sensors," in Proc. of the 11th Annual Int'l Conference on Mobile Computing and Networking (MobiCom), 2005.

[10] A. Saipulla, C. Westphal, B. Liu, and J. Wang, "Barrier coverage of line-based deployed wireless sensor networks," in IEEE INFOCOM, April 2009, pp. 127–135.

[11] S. Kumar, T. Lai, M. Posner, and P. Sinha, "Maximizing the lifetime of a barrier of wireless sensors," IEEE Transactions on Mobile Computing, vol. 9, no. 8, August 2010.

[12] H. Yang, D. Li, Q. Zhu, W. Chen, and Y. Hong, "Minimum energy cost k-barrier coverage in wireless sensor networks," in Proc. of the 5th Int'l Conf. on Wireless Alg., Systems, and Applications (WASA), 2010.

[13] H. Luo, H. Du, D. Kim, Q. Ye, R. Zhu, and J. Zhang, "Imperfection better than perfection: Beyond optimal lifetime barrier coverage in wireless sensor networks," in Proc. of The IEEE 10th Int'l Conference on Mobile Ad-hoc and Sensor Networks (MSN), December 2014.

[14] D. Li, B. Xu, Y. Zhu, D. Kim, and W. Wu, "Minimum (k,w)-angle barrier coverage in wireless camera sensor networks," Int'l Journal of Sensor Networks (IJSNET), 2014.

[15] L. Guo, D. Kim, D. Li, W. Chen, and A. Tokuta, "Constructing belt-barrier providing quality of monitoring with minimum camera sensors," in 23rd Int'l Conf. on Computer Communication and Networks (ICCCN), August 2014.

[16] B. Xu, D. Kim, D. Li, J. Lee, H. Jiang, and A. Tokuta, "Fortifying barrier-coverage of wireless sensor network with mobile sensor nodes," in Proc. of the 9th Int'l Conference on Wireless Algorithms, Systems, and Applications (WASA), June 2014.

[17] D. Kim, J. Kim, D. Li., S. S. Kwon, and A. Tokuta, "On sleep-wakeup scheduling of non-penetrable barrier-coverage of wireless sensors," in Proc. of the IEEE Global Communications Conference (GLOBECOM), December 2012, pp. 321–327.

[18] D. Kim, H. Kim, D. Li, S. S. Kwon, A. O. Tokuta, and J. A. Cobb, "Maximum lifetime dependable barrier-coverage in wireless sensor networks," Ad Hoc Networks, vol. 36, no. 1, Jan 2016.

[19] J. A. Cobb, "Improving the lifetime of non-penetrable barrier coverage in sensor networks," in IEEE 14th International Workshop on Assurance in Distributed Systems and Networks (ADSN), June 2015, pp. pp. 1–10.

[20] J. Cobb, "In defense of stint for dense breach-free sensor barriers," in Int'l Conf. on Systems and Networks Communications (ICSNC), 2017.

[21] Z. Zhang, W. Wu, J. Yuan, and D.-Z. Du, "Breach-free sleep-wakeup scheduling for barrier coverage with heterogeneous wireless sensors," IEEE/ACM Trans. on Networking, vol. 26, no. 5, 2018, pp. 2404–2413.

[22] H. Kim and J. A. Cobb, "Maximizing the lifetime of reinforced barriers in wireless sensor networks," Concurrency and Computation: Practice and Experience, vol. 29, no. 23, 2017.

 ISBN: 978-1-61208-895-2